Development 140, 2409-2421 (2013) doi:10.1242/dev.093385

Tcf21 regulates the specification and maturation of proepicardial cells

Panna Tandon[1,2], Yana V. Miteva[3], Lauren M. Kuchenbrod[1,2,4], Ileana M. Cristea[3] and Frank L. Conlon[1,2,4,*]

SUMMARY

The epicardium is a mesothelial cell layer essential for vertebrate heart development and pertinent for cardiac repair post-injury in the adult. The epicardium initially forms from a dynamic precursor structure, the proepicardial organ, from which cells migrate onto the heart surface. During the initial stage of epicardial development crucial epicardial-derived cell lineages are thought to be determined. Here, we define an essential requirement for transcription factor Tcf21 during early stages of epicardial development in *Xenopus*, and show that depletion of Tcf21 results in a disruption in proepicardial cell specification and failure to form a mature epithelial epicardium. Using a mass spectrometry-based approach we defined Tcf21 interactions and established its association with proteins that function as transcriptional co-repressors. Furthermore, using an *in vivo* systems-based approach, we identified a panel of previously unreported proepicardial precursor genes that are persistently expressed in the epicardial layer upon Tcf21 depletion, thereby confirming a primary role for Tcf21 in the correct determination of the proepicardial lineage. Collectively, these studies lead us to propose that Tcf21 functions as a transcriptional repressor to regulate proepicardial cell specification and the correct formation of a mature epithelial epicardium.

KEY WORDS: Tcf21, Proepicardial organ, Heart development

INTRODUCTION

During embryonic heart development, the formation and mitogenic growth of the heart are sustained through contribution from the epicardium, which is a specialized layer of cells derived from a mesothelial precursor structure, the proepicardial organ (PEO). Subpopulations of epicardial cells undergo epithelial-mesenchymal transition (EMT) and migrate into the sub-epicardial space and myocardium, where they differentiate into interstitial cells, cardiac fibroblasts and smooth muscle cells (reviewed by Lie-Venema et al., 2007; Ratajska et al., 2008; van Wijk et al., 2009; Pérez-Pomares and de la Pompa, 2011; Gittenberger-de Groot et al., 2012; von Gise and Pu, 2012). Moreover, during cardiac repair post-injury in the adult, epicardial cells reestablish their developmental genetic program, migrate into wounded myocardium and differentiate into the required cell lineages to provide support to regenerating heart tissue (Lepilina et al., 2006; Limana et al., 2007; Winter et al., 2007; Winter et al., 2009; Limana et al., 2010).

Basic helix-loop-helix (bHLH) transcription factors play crucial roles in cell fate specification and differentiation during organ development, including the heart (Massari and Murre, 2000; Conway et al., 2010). Transcription factor 21 (Tcf21; also known as Pod1, Epicardin, Capsulin) is expressed in the mesenchyme of developing organs, including the branchial arches, kidney, lung, spleen, gonads and in the PEO and epicardium (Lu et al., 1998; Quaggin et al., 1998; Tamura et al., 2001; Simrick et al., 2005; Serluca, 2008). *Tcf21* mouse mutants display severe developmental defects and die shortly after birth due to pulmonary hyperplasia (Quaggin et al., 1999; Lu et al., 2000). Moreover, depletion of Tcf21 leads to defects in epithelial differentiation and branching in the kidney and lung, a phenotype that is thought to arise from disrupted epithelial-mesenchymal interactions (Quaggin et al., 1999). More recently, Tcf21 function has been linked to epicardial EMT and differentiation (Acharya et al., 2012; Braitsch et al., 2012).

Here, we characterized the morphological, molecular and cellular development of the epicardium in a new vertebrate model, *Xenopus*. We further define an essential role for Tcf21 in epicardial development and show that, in the absence of Tcf21, epicardial cells fail to form a cohesive polarized sheet and instead are retained in a proepicardial (PE) precursor state. This is in contrast to recent data and thus provides unique insight into the *Tcf21*-null mouse phenotype, which may result from deleterious epicardial organization at an earlier stage of development. Using a proteomics approach we identify Tcf21 protein interactions, determining that Tcf21 associates with co-factors involved in transcriptional repression including HDAC2, Pbx1 and Ctbp2, the latter two having established requirements in cardiac development. Furthermore, using high-throughput sequencing analysis we define a unique set of nine genes that are expressed in the PEO and are repressed by Tcf21, and observe a persistent and increased expression of these markers in epicardial cells depleted of Tcf21. Altogether, our data demonstrate that Tcf21 functions as a transcriptional repressor to regulate processes of proepicardial specification and epicardial maturation.

MATERIALS AND METHODS

Cell transfection and immunoaffinity purification (IP) of Tcf21 and interaction partners

Human embryonic kidney 293 (HEK293) cells were plated onto two sets of 10×15 cm culture dishes and transfected at 40% confluence with FuGENE 6 (Roche) at a 3:1 ratio, using 20 μg EGFP control plasmid (pEGFP_N1) or Tcf21-EGFP plasmid (EGFP_N1-xlTcf21cds, NP_001085957). Cells were grown to confluence, harvested, frozen in liquid nitrogen and processed as described (Greco et al., 2011; Conlon et al., 2012). Cell powders were

[1]University of North Carolina McAllister Heart Institute, University of North Carolina at Chapel Hill, Chapel Hill, NC 27599-3280, USA. [2]Department of Genetics, University of North Carolina at Chapel Hill, Chapel Hill, NC 27599-3280, USA. [3]Department of Molecular Biology, Princeton University, NJ 08544-1014, USA. [4]Department of Biology, University of North Carolina at Chapel Hill, Chapel Hill, NC 27599-3280, USA.

*Author for correspondence (frank_conlon@med.unc.edu)

Accepted 8 April 2013

suspended in prechilled optimized lysis buffer [20 mM HEPES-KOH pH 7.4, 0.1 M potassium acetate, 2 mM $MgCl_2$, 0.1% Tween 20 (v/v), 1 μM $ZnCl_2$, 1 μM $CaCl_2$, 0.5% Triton X-100 (v/v), 150 mM NaCl, 4 μg/ml DNase, 1/100 (v/v) Protease Inhibitor Cocktail and 1/100 Phosphatase Inhibitor Cocktail] using 5 ml lysis buffer/g cell powder. Lysates were homogenized, subjected to centrifugation, and supernatants incubated for 1 hour with 7 mg magnetic beads (M270 Epoxy Dynabeads, Invitrogen) conjugated with anti-EGFP antibodies (Cristea et al., 2005). Proteins were eluted by incubation for 10 minutes (70°C) in 30 μl 1× LDS sample buffer (Invitrogen) containing 1× Reducing Agent (Invitrogen), followed by shaking at room temperature for 10 minutes.

In-solution digestion, mass spectrometry analysis and data processing

Protein IP eluates were prepared as described (Conlon et al., 2012; Greco et al., 2011; Greco et al., 2012; Tsai et al., 2012). Briefly, IP eluates were mixed with 8 M urea in aqueous 0.1 M Tris-HCl pH 8.0, applied to ultrafiltration Vivacon 500 units (Sartorius Stedim), and centrifuged at 14,000 ***g*** for 40 minutes at 20°C. Samples were washed, alkylated and digested with trypsin (Promega) overnight at 37°C. Resulting peptides were collected by centrifugation, acidified with trifluoroacetic acid, concentrated by vacuum centrifugation, and desalted using Empore C18 StageTips (Rappsilber et al., 2007; Greco et al., 2012). Peptides were analyzed by nLC-MS/MS using a Dionex Ultimate 3000 RSLC system coupled online to an LTQ-Orbitrap Velos mass spectrometer (ThermoFisher Scientific) (Greco et al., 2012; Tsai et al., 2012). Peptides were fragmented by collision-induced dissociation (CID) and the MS/MS spectra were extracted by Proteome Discoverer (ThermoFisher Scientific) and searched by SEQUEST against a database containing *Xenopus*, human and mouse UniProt Swiss-Prot sequences, including common contaminants and reversed sequences. Results were validated in Scaffold (Proteome Software) using PeptideProphet and ProteinProphet. Co-isolated proteins were considered as Tcf21-specific interactions if absent or enriched by at least 3-fold compared with controls. Proteins were clustered into functional subgroups according to biological roles based on Gene Ontology (GO) annotations.

RNA extraction and cDNA libraries

Xenopus embryos, injected with ConMO or Tcf21-MO (40 ng), were grown to stage 45. Hearts were collected (n=70-100 per condition) and processed for RNA extraction (1 μg), purified using Sera-Mag magnetic oligo(dT) beads (Thermo Scientific), fragmented to ~300 bp at 70°C for 4 minutes, and cDNA generated (Superscript II, Invitrogen). For Solexa cDNA libraries, 10 ng cDNA was blunted and paired-end adapters (Illumina/Solexa) ligated before purification on AMPure-XP (SPRI) beads (Agencourt). cDNA was amplified (PfuUltra II Fusion HS DNA polymerase, Stratagene), analyzed for purity and fragmentation size using a 2100 Bioanalyzer (Agilent) and sequenced using an Illumina Genome Analyzer II system (High-Throughput Sequencing Facility, UNC).

RNA-seq

To reduce redundancy and isolate high-quality reads, 8879 cDNA sequences annotated as RefSeq sequences in XenBase (Bowes et al., 2008) (May, 01, 2011) were used for expression analysis (http://www.marcottelab.org/index.php/Xenopus_reference; Taejoon Kwon, Marcotte lab., University of Texas, Austin). Alignments were performed on Bowtie2 v2.0.0.6 (Johns Hopkins University) and normalized for total counts to determine fold change between control and Tcf21-depleted cardiac cDNA datasets (GEO series GSE45786). Secondary screens were based on fold change (see supplementary material Table S3) and GO term analysis performed using GOrilla (updated 12/08/2012) (Eden et al., 2007; Eden et al., 2009) (see supplementary material Tables S1 and S2) and ReviGO (updated 04/02/2012) (Supek et al., 2011), and validated using RT-PCR from independent biological replicates (supplementary material Table S4, Fig. S7).

Xenopus transgenics

Linearized DNA (CMV:dsRED, *Not*I; gift from Enrique Amaya, Manchester University, UK) and CAG:KikumeGR (*Sal*I) (Nowotschin and Hadjantonakis, 2009) were introduced into *Xenopus* using trangenesis procedures (Kroll and Amaya, 1996; Mandel et al., 2010). Fluorescent embryos were sorted and housed until adulthood, when germline transmission was tested. Stage 39-40 CAG:KikumeGR transgenic embryos were placed in low-melting-point agarose (0.8%) in 0.33× Marc's Modified Ringer's (MMR) cooled to room temperature. Embryos were positioned ventral side down on a coverslip-based dish in agarose, submerged in 0.1× Modified Barth's Saline (MBS) containing 0.01% tricaine. Localized bleaching of the septum transversum (ST) was performed using a UV laser (Zeiss 710 confocal, seven cycles, 100 iterations, scan speed 10, excitation 405 nm at 100%). Embryos were excised and recovered in 0.1× MBS before imaging (Leica MZ16F, Retiga 4000RV camera) (supplementary material Fig. S1).

Xenopus manipulations

Xenopus embryos were staged according to Nieuwkoop and Faber (Nieuwkoop and Faber, 1967; Brown et al., 2005). An EST cDNA IMAGE *X. laevis* clone (ID 8077326, Open Biosystems) was sequenced and identified as full-length *Tcf21* (Simrick et al., 2005). Two non-overlapping translation-blocking morpholinos (MOs) were designed against the start site of *Tcf21* and upstream 5′UTR region (Tandon et al., 2012) as determined by RLM-RACE (Invitrogen, Gene Tools) (supplementary material Fig. S3); 40 ng Tcf21-MO1 and Tcf21-MO2 were injected at the one-cell stage (Tandon et al., 2012) (see supplementary material Table S5 for MO sequences).

In situ hybridization

Whole-mount *in situ* hybridization (ISH) was carried out as described (Harland, 1991), the pericardial cavity membrane in late tadpole stage embryos being removed postfixation to improve resolution. Embryos were processed for vibratome sectioning (30 μm) (Gessert and Kühl, 2009). The *Wt1* probe was kindly provided by Peter Vize (Carroll and Vize, 1996); all other probes were generated by PCR (supplementary material Table S6) or reported previously (Brown et al., 2005; Goetz et al., 2006; Langdon et al., 2007).

Immunohistochemistry

Antibody staining was conducted as reported (Brown et al., 2005; Christine and Conlon, 2008; Mandel et al., 2010; Langdon et al., 2012) (supplementary material Table S7), then incubated in DAPI (200 ng/ml in PBS) and processed for agarose vibratome sectioning (150-200 μm) (Wallingford, 2010) or cryosectioning (10 μm) (Brown et al., 2005). Images were taken on an Olympus IX 81-ZDC inverted fluorescence microscope or Zeiss LSM710.

Electron microscopy

The pericardial cavity membrane was excised from embryos anaesthetized in 0.1% (w/v) tricaine and transmission (TEM) and scanning (SEM) electron microscopy conducted as reported using a Zeiss EM 910 and a Zeiss Supra 25 FESEM, respectively (Microscope Services Laboratory, UNC) (Brown et al., 2007).

Live imaging of epicardial explants

Stage 40 embryos were incubated in 0.1× MBS containing 25 μg/ml gentamycin and 0.1% iodine for 2 hours at room temperature, and subsequently maintained in 0.1× MBS containing 0.006% iodine and 25 μg/ml gentamycin. Rat tail collagen I [3 mg/ml collagen I, 40 mM sodium bicarbonate in 1× Dulbecco's Modified Eagle Medium (DMEM) pH 8, on ice] was added at 10 μl per well of a 24-well plate, and allowed to gel at room temperature for 30 minutes. Wells were rinsed with 1× Barth's solution and incubated with Barth's$^+$ (70 μg/ml gentamycin, 50 U/ml nystatin, 0.006% iodine and 10% heat-inactivated fetal bovine serum), rocking for 1 hour at room temperature. Hearts were excised from anaesthetized embryos and placed in Barth's on 1% agarose dishes on ice, then placed onto air-dried collagen cushions and allowed to adhere for 20 minutes at room temperature before the addition of Barth's$^+$, then cultured at 23°C in a humidified chamber for 24-48 hours, fixed in 4% paraformaldehyde and processed for immunostaining as described, or visualized on an Olympus IX70. Live images were captured every 30 minutes over a 24- to 48-hour period at room temperature and analyzed

using ImageJ (NIH) and Imaris (Bitplane) software. Double-transgenic embryos (CMV:dsRED, CA:GFP) were used to enable better visualization and cell migration tracking by Imaris software (supplementary material Fig. S9). Two-tailed unpaired non-parametric Mann-Whitney statistical test was used to determine significance (GraphPad Prism 6, JMP).

RESULTS

Conserved epicardial development in *Xenopus*

To gain new insights into the essential role of the epicardium during development, we turned to a non-mammalian vertebrate model system that is highly effective for modeling cardiac development. Molecular mechanisms of heart development in the frog *Xenopus* are highly conserved with those of mouse and human (Brown et al., 2003; Gormley and Nascone-Yoder, 2003; Mohun et al., 2003; Brown et al., 2005; Garriock et al., 2005; Goetz et al., 2006; Bartlett et al., 2007; Langdon et al., 2007; Warkman and Krieg, 2007; Bartlett and Weeks, 2008; Afouda and Hoppler, 2009; Evans et al., 2010; Mandel et al., 2010; Kaltenbrun et al., 2011; Langdon et al., 2012). We have confirmed that, similar to other vertebrates, *Xenopus* epicardium develops as a specialized layer of cells surrounding the heart and is derived from a mesothelial precursor structure, the PEO, located on the ST (Jahr et al., 2008). SEM analysis of *Xenopus* verifies that by late tadpole stages – roughly equivalent to E9.5 in mouse, HH17 in chick and day 20 in human embryonic development – the precursor epicardial structure and epicardium display prominent phenotypic changes as they migrate onto and over the ventricular surface (supplementary material Fig. S1) (Jahr et al., 2008). The PEO forms on the right-hand side on the ST and attaches to the heart at the atrioventricular sulcus (AVS) close to the outflow tract (OFT) junction by stage 41 (supplementary material Fig. S1B-D) (Jahr et al., 2008). Interestingly, at these stages this region of the *Xenopus* heart expresses BMP2 (supplementary material Fig. S1K-P), a factor shown to influence correct PEO attachment and migration (Ishii et al., 2010). At slightly later stages, the PEO bridge is maintained (supplementary material Fig. S1D) and the epicardium develops as a distinct smooth epithelial-like sheet that gradually progresses over the cobblestone-like cardiac surface (supplementary material Fig. S1C-F) (Jahr et al., 2008). To confirm that cells of the *Xenopus* PEO are similar to those of mammals and undergo similar cell movements, we generated transgenic *Xenopus* embryos ubiquitously expressing the photoconvertible fluorescent protein KikumeGR (Nowotschin and Hadjantonakis, 2009; Griswold et al., 2011; Ridelis et al., 2012). Photoconversion of cells within the ST and PEO (stage 39/40) confirms that these cells migrate, attach and form an epicardial sheet over the surface of the heart (stage 43, supplementary material Fig. S1G-J).

To determine whether the molecular underpinnings of epicardial development are conserved in *Xenopus*, we examined expression patterns of the epicardial-associated transcription factors Tbx18 (Kraus et al., 2001; Begemann et al., 2002; Haenig and Kispert, 2004; Jahr et al., 2008), Wilm's tumor 1 (Wt1) (Moore et al., 1998; Carmona et al., 2001) and Tcf21 (Quaggin et al., 1998; Simrick et al., 2005; Ishii et al., 2007; Serluca, 2008) (Fig. 1). We observed that all three are evolutionarily conserved in expression with regards to the ST/PEO and epicardium. However, we also note a distinct spatiotemporal discrepancy, with Tbx18 being expressed in the ST first (stage 31-32, Fig. 1A), followed by Wt1 and Tcf21 (stage 36, Fig. 1E,F), suggesting a potential hierarchical organization of these genes or subfunctionalization within the PEO, as postulated in mouse and chick (Mikawa and Gourdie, 1996; Braitsch et al., 2012). Expression of these markers becomes more spatially restricted to the PEO at later stages, prior to migration onto the heart (stage 40, Fig. 1G-L), with Tcf21 displaying a more confined distribution (Fig. 1H,K). Thus, the cellular and molecular hallmarks of epicardium formation are conserved from *Xenopus* to mouse.

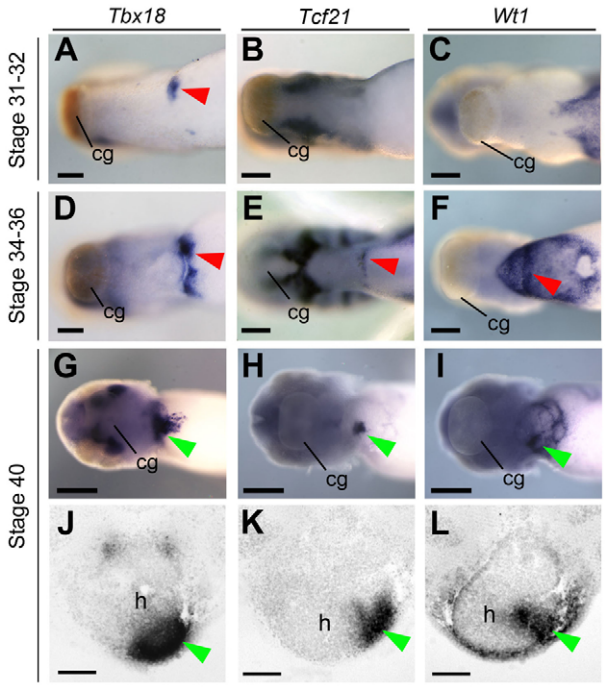

Fig. 1. Conservation of epicardial markers in *Xenopus*. (**A-L**) *In situ* hybridization (ISH) for *Tbx18* (A,D,G,J), *Tcf21* (B,E,H,K) and *Wt1* (C,F,I,L) in developing *Xenopus* embryos, showing ventral views of the anterior region (anterior left) (A-I) or transverse vibratome sections through the heart (anterior top) (J-L). *Tbx18* expression was observed in the septum transversum (ST) (red arrowheads in A,D) earlier than that of *Tcf21* (red arrowhead in E) and *Wt1* (red arrowhead in F). Expression of all genes becomes restricted to proepicardial organ (PEO) by stage 40 (green arrowheads in G-L). cg, cement gland; h, heart. Scale bars: 2 mm in A-I; 100 µm in J-L.

Tcf21 is required for epicardial attachment

Since studies have reported that null mutations in *Tbx18* have little effect on epicardial development (Bussen et al., 2004; Christoffels et al., 2006), we sought to establish the function of Wt1 and Tcf21 during this process in *Xenopus*. Consistent with studies in mouse (Martínez-Estrada et al., 2010; Moore et al., 1999), depletion of Wt1 in *Xenopus*, although resulting in severe pericardial edema, did not affect initial PEO outgrowth, migration or formation of the epithelial epicardial sheet (supplementary material Fig. S2). By contrast, we observed an essential requirement for Tcf21 in *Xenopus* epicardium formation. Marker analysis showed that Tcf21 is not essential for the initiation of cardiac mesoderm (supplementary material Fig. S3) or PEO specification because *Tcf21*, *Wt1* and *Tbx18* expression is detected and maintained in Tcf21-depleted embryos (see Fig. 7S-V; data not shown). Detailed ultrastructural analysis using SEM and TEM confirmed the presence of a PEO in Tcf21-depleted embryos and further indicated that cells from the PEO were able to traverse onto the myocardial surface between stages 41 and 43 (Fig. 2). Strikingly, at stage 44 the epicardial layer of Tcf21-depleted embryos lacked adhesive connections to the underlying myocardium (Fig. 2Q-T′) and epicardial cells displayed a more rounded, bleb-like morphology as compared with the smooth

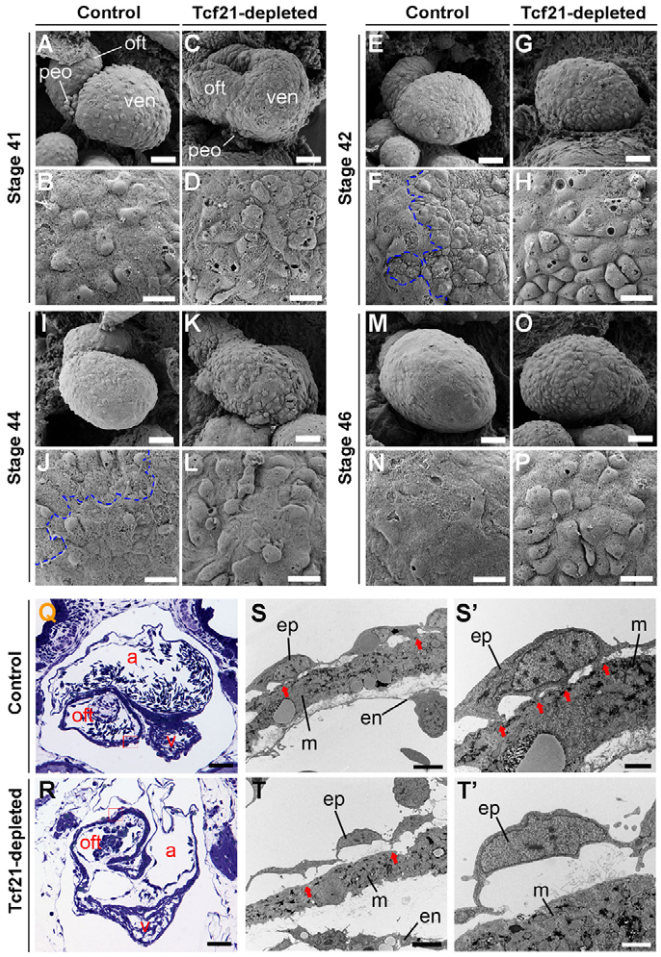

Fig. 2. Tcf21 is required for epicardial integrity and adhesion to the myocardial surface. (**A-P**) SEM images of hearts from control and Tcf21-depleted *Xenopus* embryos (A,C,E,G,I,K,M,O) with magnified views of the ventricular region (B,D,F,H,J,L,N,P). Blue dashed line indicates the extent of epicardial sheet migration over the ventricular surface. Ventral views of pericardial cavity with anterior at top (A-P). (**Q-T′**) Toluidine Blue staining (Q,R) (dorsal at top) and TEM images (S-T′) of transverse sections through the heart region demonstrating adhesions, or lack thereof, to the underlying myocardial surface (red arrows). The boxed regions in Q,R are magnified in S-T′. a, atrium; en, endocardium; ep, epicardium; m, myocardium; oft, outflow tract; peo, proepicardial organ; v/ven, ventricle. Scale bars: 50 μm in A,C,E,G,I,K,M,O; 25 μm in B,D,F,H,J,L,N,P; 5 μm in S,T; 2 μm in S′,T′.

epithelial sheet in controls (Fig. 2I-P; supplementary material Fig. S1). Collectively, these data define a requirement for Tcf21 for correct epicardial layer morphology and the ability of the epicardium to adhere to the myocardial surface of the heart.

Tcf21 associates with repressor complex proteins and is phosphorylated at multiple sites

Our findings are consistent with an evolutionarily conserved role for Tcf21 in epicardium formation. However, the molecular mechanisms by which Tcf21 acts to regulate transcription are yet to be established. Therefore, we sought to determine the general transcription factor complex proteins that interact with Tcf21. We used immunoaffinity purification (IP) and quantitative mass spectrometry to characterize Tcf21 interactions (Fig. 3A). Optimization of IP conditions [performed as described (Conlon et al., 2012; Greco et al., 2011; Tsai et al., 2012)] allowed us to successfully isolate transfected EGFP-tagged *Xenopus* Tcf21 from HEK293 cells (Fig. 3B; supplementary material Fig. S4, Table S8). In the absence of a confirmed cardiac/epicardial cell line, the HEK293 cell line was chosen to perform this screen as it endogenously expresses Tcf21 and is routinely used to study Tcf21 transcriptional activity. Interestingly, epicardial and nephric tissue may share an evolutionary origin and therefore have conserved mechanisms of transcriptional regulation (Pombal et al., 2008) (see Discussion). This approach is supported by the observation that the C-terminal EGFP tag on Tcf21 has little or no effect on Tcf21 activity in bioassays (e.g. injection of EGFP-tagged Tcf21 into *Xenopus* gives the same phenotype as control Tcf21, data not shown).

As expected, among the proteins unique to the Tcf21 isolation versus the control IP was the transcriptional regulator Tcf12 (supplementary material Fig. S4A), a known Tcf21 heterodimerization partner (Hidai et al., 1998; Lu et al., 1998; Arab et al., 2011). Interestingly, our results from two biological replicate experiments identified an association of Tcf21 with HDAC2 (supplementary material Fig. S4B-D), a class I histone deacetylase involved in transcriptional regulation and chromatin remodeling, as well as with the pre-B-cell leukemia transcription factor 1 (Pbx1), which is known to be crucial in cardiovascular development (Chang et al., 2008). In addition, C-terminal-binding protein 2 (Ctbp2) was identified, a protein that is involved in BH3-only gene expression, p53-independent apoptosis, as well as cardiac development and transcriptional repression via interaction with the E1A and E-box repressor ZEB (Hildebrand and Soriano, 2002; Zhao et al., 2006; Kovi et al., 2010). The Ctbp2 interaction with Tcf21 was validated by independent immunoaffinity isolation (Fig. 3C; supplementary material Fig. S4C). GO analysis of putative Tcf21 interactions also highlighted proteins involved in DNA repair: RecQl, Lig3 and Msh6 (Fig. 3E; supplementary material Table S8). All genes isolated were identified in *Xenopus* cardiac tissue by RNA-seq analysis and hence corroborate a potential conservation of Tcf21 transcriptional regulation and protein interactions (Fig. 3D).

The IP of Tcf21 further provided an enrichment that allowed the identification of previously unreported post-translational modifications on Tcf21. Within the 59% amino acid sequence coverage obtained, three phosphorylation sites were identified with high confidence on Tcf21 on the serine residues S37, S48 and S67 (Fig. 3F; supplementary material Figs S5 and S6). Interestingly, Tcf21 phosphorylation sites were localized within the N-terminal region (Fig. 3F; supplementary material Fig. S5A-E, Fig. S6) on residues that are evolutionarily conserved across species, implying a functional role for these post-translational modifications.

Identification of unique PE genes

Having established that Tcf21 is required for PEO/epicardium formation and can interact with transcriptional co-repressors, we sought to identify genes downregulated by Tcf21 during epicardial development using high-throughput sequence analysis to determine the cardiac transcriptome in Tcf21-depleted embryos versus controls (stage 45, supplementary material Fig. S1; Fig. 2). Consistent with our proteomic data we observed a trend whereby the 146 genes that were upregulated at least 1.8-fold (supplementary material Tables S8-S10) were significantly enriched for functions involving extracellular matrix (ECM), cell adhesion and locomotion by GO term analysis (GOrilla), in concurrence with cellular processes known to be involved with epicardium formation (Kálmán et al.,

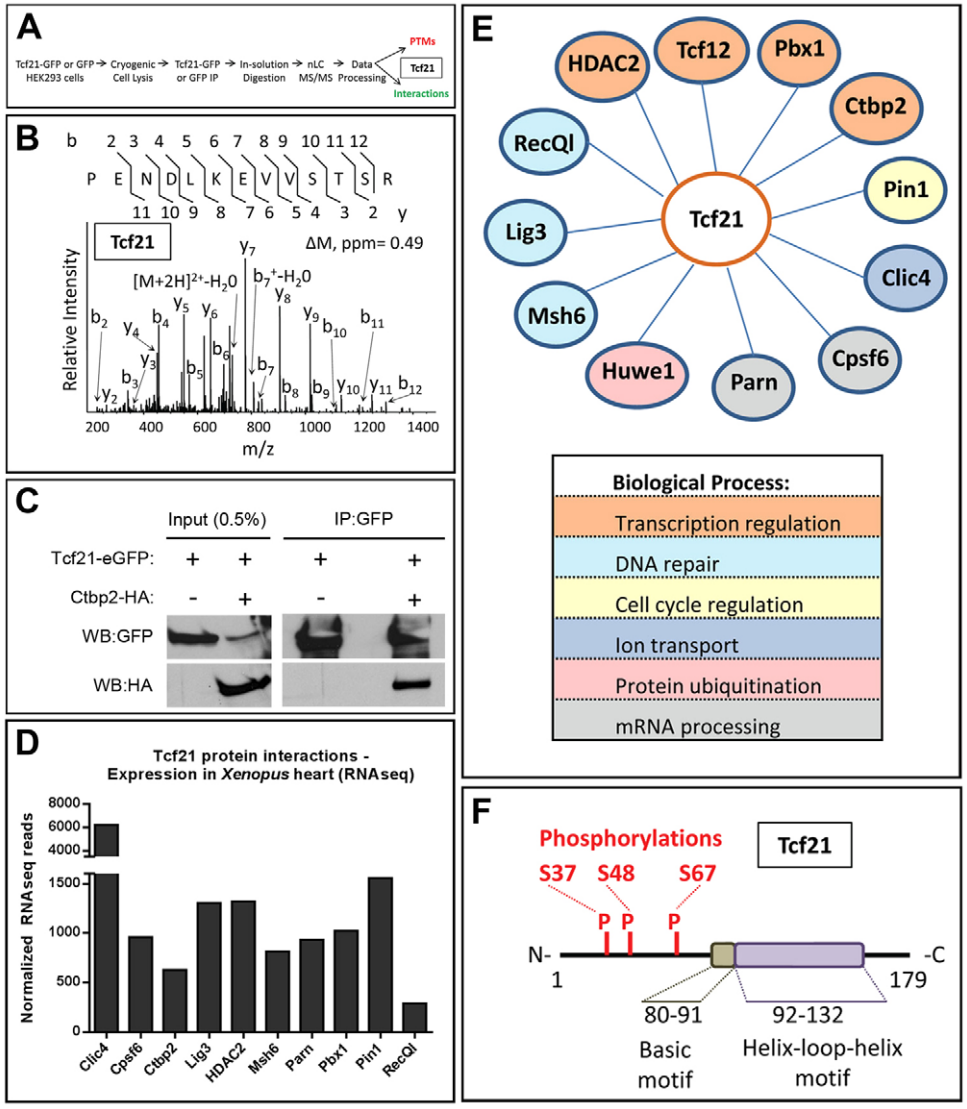

Fig. 3. Tcf21 associates with co-repressor proteins and is phosphorylated at multiple sites. (**A**) Experimental workflow for Tcf21 immunoaffinity purification (IP), and identification of Tcf21 interactions and post-translational modifications (PTMs). (**B**) Identification of Tcf21 peptide by CID MS/MS analysis. 'ΔM, ppm' refers to the difference between experimental and theoretical peptide masses in parts per million. (**C**) IP validation of interaction between Tcf21 and Ctbp2 in HEK293 cells. Both proteins run at ~50 kDa. WB, western blot. (**D**) Expression of Tcf21 protein interaction candidates, as identified by mass spectrometry, in *Xenopus* stage 45 cardiac tissue analyzed by RNA-seq read counts. Huwe1 and Tcf12 were not included in the RefSeq library used for alignment. (**E**) Enriched putative Tcf21 interactions, color-coded according to their GO annotations for biological processes. (**F**) Map of identified Tcf21 phosphorylation sites on serine residues.

1995; Nahirney et al., 2003; Hirose et al., 2006; Pae et al., 2008; Martínez-Estrada et al., 2010) (supplementary material Fig. S7A).

Top candidate genes were validated by RT-PCR from independent biological replicates (supplementary material Fig. S7B, Table S9) and whole-embryo spatiotemporal expression analysis by ISH (Fig. 4; supplementary material Table S10). Candidate genes were selected based on potential roles during epicardial development, cell adhesion, migration or interactions with the ECM. From the 25 genes analyzed by ISH, 15 out of 18 genes from the upregulated dataset showed increased expression throughout the embryo, with 12 genes displaying augmented expression in the PEO and migrating epicardial cells in control and Tcf21-depleted embryos, therefore identifying nine genes as unique markers of the PEO (Fig. 4A-P,CC,DD; supplementary material Table S10). From the downregulated gene set, of the seven genes examined by ISH only one showed expression in the PEO: *PDGFRα*, a known epicardial marker (Kang et al., 2008).

A subset of the upregulated genes was analyzed further by ISH at earlier stages to validate them as PE cell markers. At these stages of epicardial development we detected a punctate region of expression using these markers, bearing close resemblance to Tcf21 expression (Fig. 4Q-FF) and therefore clarifying them as markers of PE cells. Significantly, at both early and later stages of epicardial development (stage 40 PEO attachment and stage 45 epicardial layer formation) we detected an expansion in PE marker expression in the absence of Tcf21 function (Fig. 4). This suggests that Tcf21 functions within a transcriptional pathway as a repressor to regulate either the transcription of PE genes or the specification of the precursor PE cells at the initial stages of epicardial development. This is in contrast to Tcf21 functioning during later processes of epicardial-derived cell (EPDC) EMT or differentiation, as has been proposed in the mouse model (Acharya et al., 2012; Braitsch et al., 2012).

Tcf21 is required for epicardial maturation

Our TEM and SEM analysis and transcriptional profiling of Tcf21-depleted cardiac tissue are all consistent with Tcf21 being required for PEO maturation. One of the hallmarks of PE maturation is the transition to a more epithelial character. Consistently, we find that Tcf21 depletion leads to a dramatic increase in the mesenchymal marker vimentin (stage 46; Fig. 5C-D″) (Dent et al., 1989; Torpey et al., 1992; Shook and Keller, 2003; Compton et al., 2006; Ramos et al., 2010; Smith et al., 2011), in line with a failure of Tcf21-depleted cells to undergo epithelialization. We further observe alterations in the

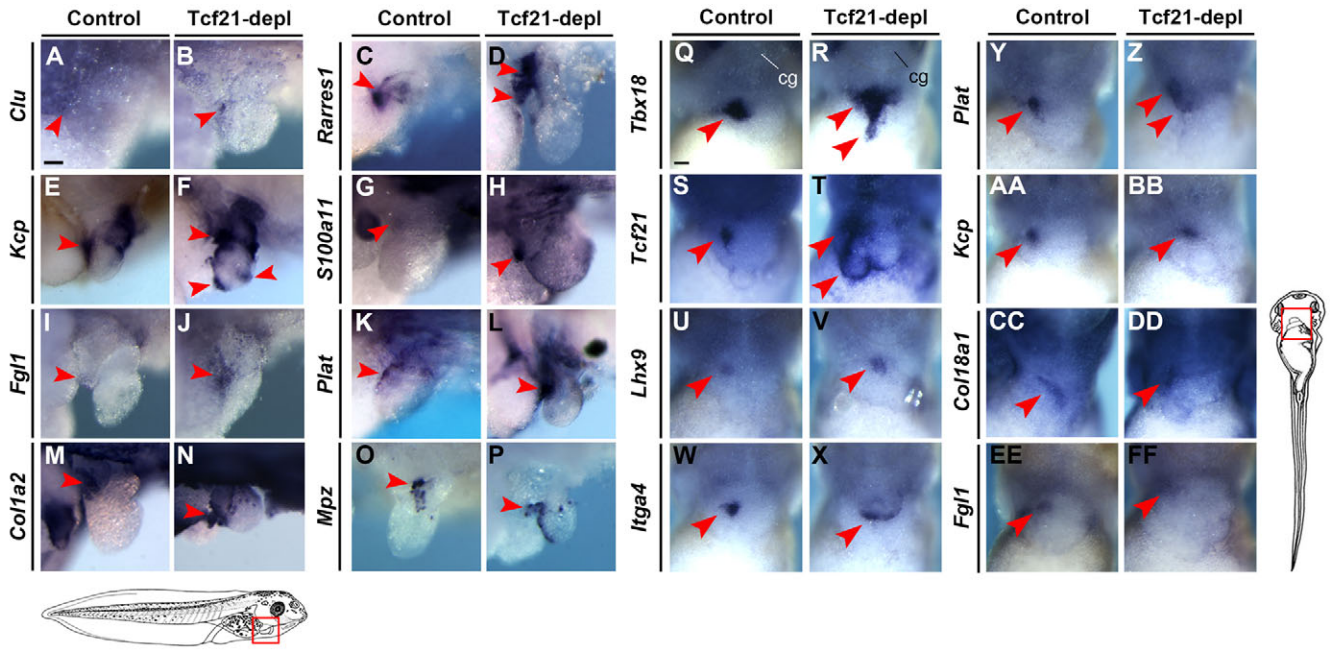

Fig. 4. Markers of epicardial precursor cells identified by high-throughput sequence analysis. (**A-P**) ISH of selected genes from the RNA-seq upregulated dataset showing expression within the PEO (arrowheads). Magnified lateral images of the heart region are shown (anterior right). (**Q-FF**) ISH of unique and known PE cell markers showing conserved expression patterns at earlier stages (stage 40) of epicardial development (ventral views, anterior top). cg, cement gland. Scale bars: 1 mm.

apical-basal polarity of Tcf21-depleted epicardial cells, as visualized by expression of the apical marker atypical protein kinase C ζ (aPKC) (Izumi et al., 1998; Hirose et al., 2006; Ghosh et al., 2008; Munson et al., 2008) (Fig. 5A-B″). Specifically, aPKC is localized along the apical aspect of the epicardium and shows sparse intracellular staining in control epicardial cells. By contrast, Tcf21-depleted cells, while retaining a degree of staining along the apical aspect, also displayed a distinct and dramatic accumulation of aPKC within cell stroma and to some extent in the nuclei (Fig. 5B′,B″), which resembles the aPKC distribution in the attached PEO (supplementary material Fig. S8). These findings were further verified by laminin staining, which was used to visualize the distribution of this basally localized protein in the fully polarized epicardial sheet on the surface of control myocardium (Fig. 5E-E″). Concomitantly, we observed alterations in this basal membrane marker in Tcf21-depleted hearts, where it displayed discontinuous staining, appearing as accumulated deposits and, in some instances, in sparse contact with the underlying myocardium (Fig. 5F-F″).

Collectively, these data indicate that Tcf21 is required for the integrity of the polarized epithelial epicardial layer, further corroborating that, in the absence of Tcf21, epicardial cells remain in the mesothelial state associated with migratory precursor PE cells.

Tcf21 depletion leads to retention of the migratory precursor state

The inability of Tcf21-depleted epicardial cells to properly adhere or form a polarized epithelium showed that Tcf21 is required for the initiation of proper epicardial integrity and, ultimately, the formation of a mature epicardium. Our observations in *Xenopus* (supplementary material Fig. S1B; Fig. 2A,C) and those from other vertebrate models (Komiyama et al., 1987; Kálmán et al., 1995; Nahirney et al., 2003; Schulte et al., 2007; Jahr et al., 2008; Serluca, 2008; Liu and Stainier, 2010) have identified PE cells as having a rounded clustered morphology that is indicative of mesenchymal characteristics that are functionally linked to their ability to migrate onto the heart surface.

We sought to directly assess the migratory potential of Tcf21-depleted epicardial cells to confirm their precursor PE cell-like phenotype. We developed a novel *Xenopus* quantitative cardiac explant assay to monitor epicardial cell behavior and allow accurate visualization of epicardial cells. For these studies we generated a new *Xenopus* transgenic line that ubiquitously expresses stable dsRED, and crossed this line with the transgenic line cardiac actin:GFP (Latinkić et al., 2002), from which double-transgenic hearts were excised at the stage when we first observed the epicardial defect in Tcf21-depleted embryos (Fig. 6; supplementary material Fig. S9). Explants were cultured on a collagen gel matrix, allowing epicardial cells to migrate off the ventricular surface. Migrating epicardial cells were analyzed for cell trajectory, cell velocity and distance traveled over a 48-hour period. From these analyses, we observed a dramatic increase in the migratory speed of Tcf21-depleted epicardial cells relative to controls (n=1382 control cells versus n=3329 Tcf21-depleted cells, three independent experiments, P<0.0001). Moreover, Tcf21-depleted epicardial cells were able to migrate a greater distance (n=29 control hearts versus n=28 Tcf21-depleted hearts, three independent experiments, P<0.0001) and showed an enrichment in F-actin stress fibers near the heart, which is indicative of a more migratory state (Fig. 6; supplementary material Movies 1 and 2, Fig. S10). However, epicardial cells derived from control and Tcf21-depleted embryos were indistinguishable in their cellular trajectory. Thus, Tcf21 is required for the molecular and cellular events associated with PE cell maturation.

Tcf21 is required for proepicardial specification

Our data thus far have implied that Tcf21 depletion results in increased detection of PE cell markers on the heart surface as well as

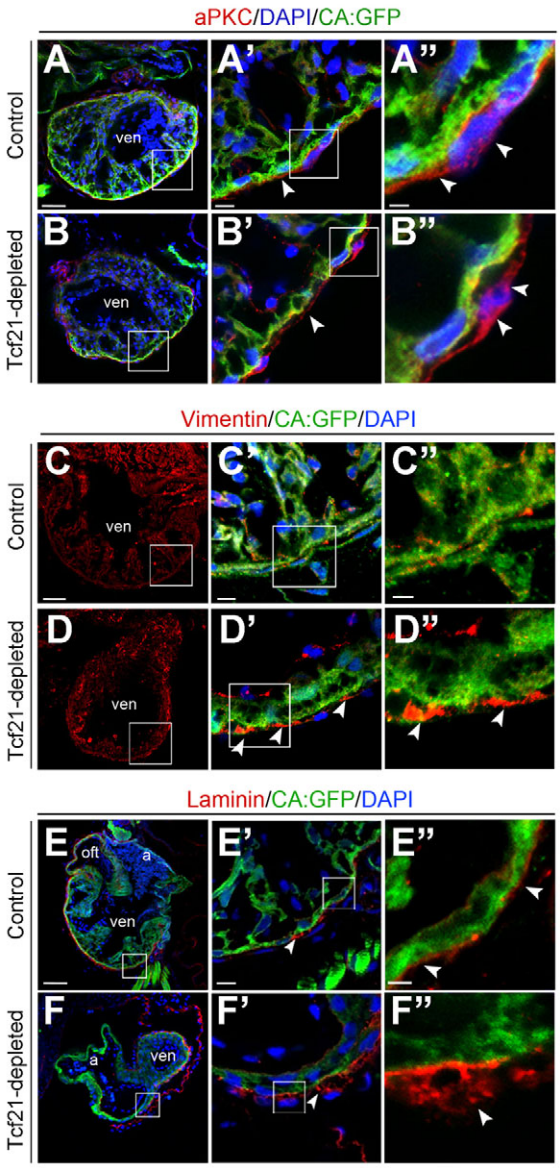

Fig. 5. Tcf21 functions to promote epicardial maturation and epithelialization. Transverse sections (dorsal to the top) through the cardiac region of stage 46 CA:GFP transgenic embryos showing myocardium (green), cell nuclei stained with DAPI (blue) and immunohistochemical stains for (**A-B″**) aPKC, (**C-D″**) vimentin and (**E-F″**) laminin in red. Arrowheads highlight epicardial cells with increased or mislocalized staining compared with controls. Boxes indicates the regions magnified in A′-F′ and A″-F″. a, atrium; oft, outflow tract; ven, ventricle. Scale bars: 50 µm in A,C,E; 10 µm in A′,C′,E′; 5 µm in C″; 2.5 µm in A″,E″.

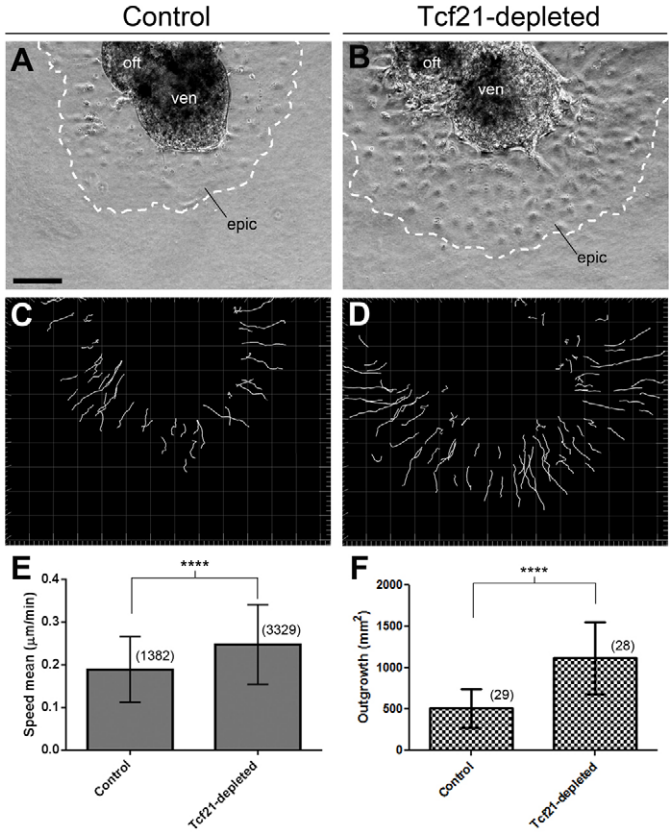

Fig. 6. Epicardial cell migration is regulated by Tcf21. (**A**,**B**) Brightfield images of control (A) and Tcf21-depleted (B) cardiac explant on collagen gel. The dashed line indicates the extent of epicardial outgrowth after 16 hours of culture. (**C**,**D**) Imaris tracking software depicts individual epicardial cell movements during culture, comparing control (C) and Tcf21-depleted (D) epicardial behavior. (**E**,**F**) A significantly increased rate of epicardial cell migration (E) and total cell outgrowth (F) in a 48-hour culture period was observed in Tcf21-depleted as compared with control embryos. ****P<0.0001, two-tailed unpaired non-parametric Mann-Whitney test. Mean ± s.d. from a total of three independent experiments with the number of (E) migrating cells from 27 control and 34 Tcf21-depleted explants or (F) hearts assayed indicated in parentheses. epic, epicardial cells; oft, outflow tract; ven, ventricle. Scale bar: 200 µm.

epicardial cells that are more rounded, more migratory and exhibit little resemblance to the polarized epithelial epicardial layer that we observe in control embryos. These characteristics are all reminiscent of the precursor PE cells as they initially migrate onto the surface of the heart. To assess whether Tcf21 is involved in the retention or increased specification of PE cells we assessed additional known markers of the PEO. LIM homeobox 9 (Lhx9) and Integrin alpha 4 (Itga4) have both been associated with epicardial development, interestingly with Lhx9 expression being specifically downregulated as the epicardial layer matures (Pinco et al., 2001; Dettman et al., 2003; Kirschner et al., 2006; Smagulova et al., 2008). Both *Lhx9* and *Itga4* were found to be upregulated in our high-throughput sequence analysis of the Tcf21-depleted cardiac transcriptome as compared with controls (3.77-fold and 2.79-fold, respectively), and whole-embryo ISH showed increased expression specifically in the area of PEO attachment to the heart in Tcf21-depleted embryos, suggesting an increased PE cell specification (Fig. 7G-J′). This was corroborated with cytokeratin staining, a marker of intermediate filaments and cells of the PEO (Vrancken Peeters et al., 1995), which was visualized in a punctate manner in the precursor PEO structure but found to be maintained in Tcf21-depleted epicardial cells migrating onto the heart surface, although only detected in the attached PEO cells in controls (Fig. 7A-F‴). These findings corroborate that migrating Tcf21-depleted epicardial cells retain a PEO-like state.

Since it is possible to analyze the spatiotemporal expression of *Tcf21* RNA in embryos depleted of Tcf21 protein by translation-blocking MOs, we further validated the role of Tcf21 in promoting epicardial maturation. In control embryos during epicardial development, Tcf21 expression was undetectable as epicardial cells migrated over the heart surface from the attached PEO to

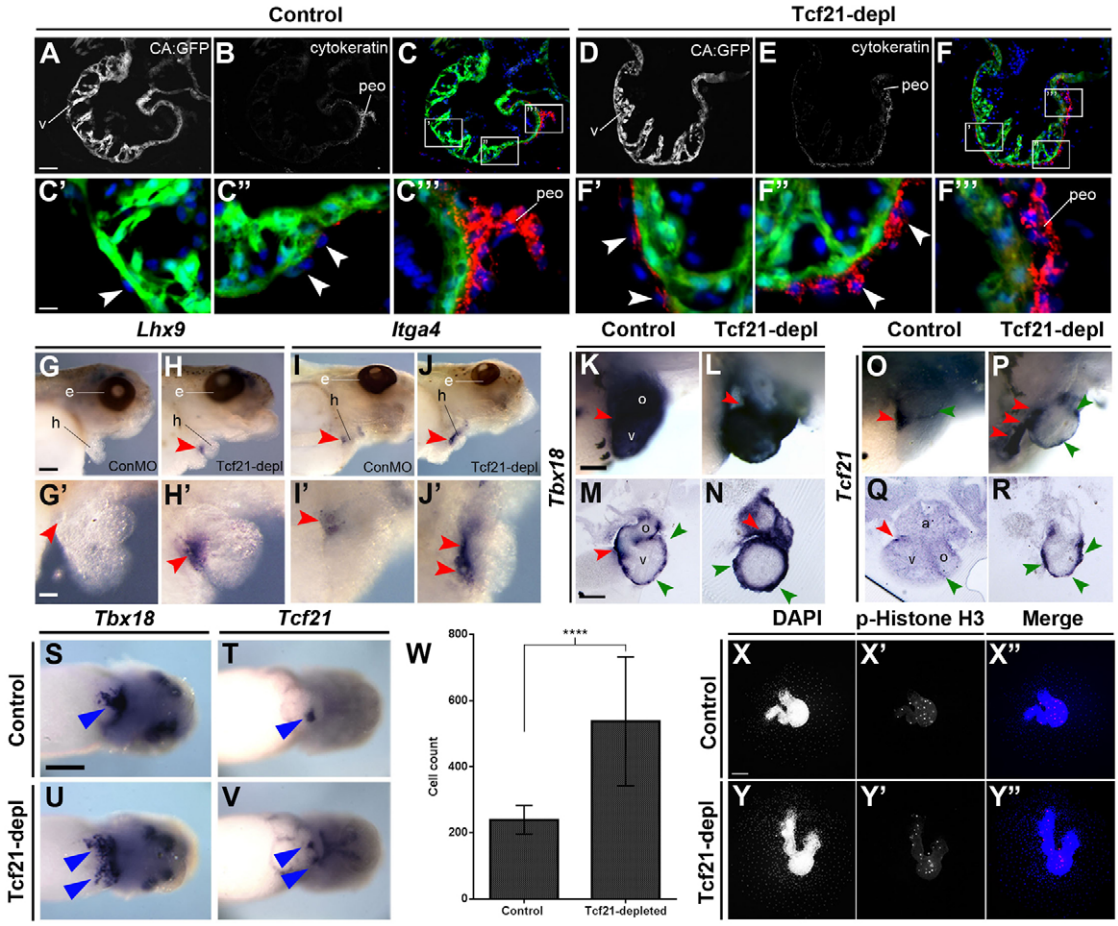

Fig. 7. Tcf21 is required for correct specification of precursor PE cells and for epicardial maturation. (**A-F″**) Transverse sections through the cardiac region of stage 46 CA:GFP transgenic *Xenopus* embryos stained for cytokeratin (red) and with DAPI (blue), with the myocardium expressing GFP under the cardiac actin promoter. Punctate cytokeratin staining is observed in migrating PE cells (arrowheads). (**G-J′**) ISH of stage 46 embryos showing the PEO markers (red arrowheads) *Lhx9* and *Itga4*; lateral views with head facing right. G′-J′ are magnifications from G-J. (**K-R**) ISH of *Tbx18* and *Tcf21* in stage 46 embryos, showing lateral magnified views of hearts (K,L,O,P; anterior right) and transverse gelatin vibratome sections (M,N,Q,R; dorsal to top). Red arrowheads indicate PEO expression, green arrowheads migrating epicardial cell expression. Note the thickened and more rounded appearance of the Tbx18-expressing layer in Tcf21-depleted embryos (N). (**S-V**) ISH of *Tbx18* and *Tcf21*; ventral images of younger, stage 40 embryos (anterior right). Arrowheads indicate PEO expression and duplication/expansion thereof in Tcf21-depleted embryos (U,V). (**W**) The number of migrating epicardial cells from Tcf21-depleted cardiac explants (17 control hearts, 23 Tcf21-depleted hearts, two independent experiments) is significantly increased compared with control (****P<0.0001, two-tailed unpaired non-parametric Mann-Whitney test). Mean ± s.d. (**X-Y″**) The increased number of DAPI-stained nuclei in Tcf21-depleted explants, compared with controls, is not due to an increase in proliferation as shown by the absence of phospho-Histone H3 staining. a, atrium; oft, outflow tract; peo, proepicardium; v, ventricle. Scale bars: 50 μm in A; 10 μm in C′; 500 μm in K; 100 μm in M; 2 mm in G,S; 1 mm in G′,X.

form the mature epithelial epicardial layer (as indicated by Tbx18 expression, Fig. 7K-N), while being retained in the attached precursor structure, suggesting that Tcf21, like Lhx9, is a marker of the precursor PEO structure (Fig. 7O,Q). Similarly, *Tcf21*, as detected by ISH, appeared to decrease as the epicardial layer matures in mouse from E11.5-E15.5 (Acharya et al., 2012). Strikingly, in Tcf21-depleted embryos, Tcf21 expression was more evident as epicardial cells covered the ventricular surface (Fig. 7P,R). These data strongly suggest that, in the absence of Tcf21, PEO cells maintain their immature characteristics as they migrate over the heart. Furthermore, the fact that Tcf21-depleted epicardial cells are unable to mature into an epicardial layer implies that Tcf21 has a role in restricting the specification of proepicardial cells. Moreover, and consistent with the expansion or duplication of the PEO region of expression at earlier stages (Fig. 4Q-FF; Fig. 7S-V), we observed a statistically higher number of migrating epicardial cells from Tcf21-depleted hearts versus controls (Fig. 6E; Fig. 7W), which is indicative of an increased number of precursor cells. This increase was not due to an increase in the mitotic index as judged by phospho-Histone H3 staining (Fig. 7X-Y″).

The data presented here therefore show an increased number of proepicardial-like cells on the heart surface in Tcf21-depleted embryos, as identified by previously known and novel PEO genes identified in this study, and thus imply a role for Tcf21 in regulating, most likely restricting, the specification of the PEO at earlier stages of epicardial development (Fig. 8).

DISCUSSION

This study has characterized in detail the dynamic transformations that are involved during the formation of the crucially important epicardial cell layer. This structure forms from a source of

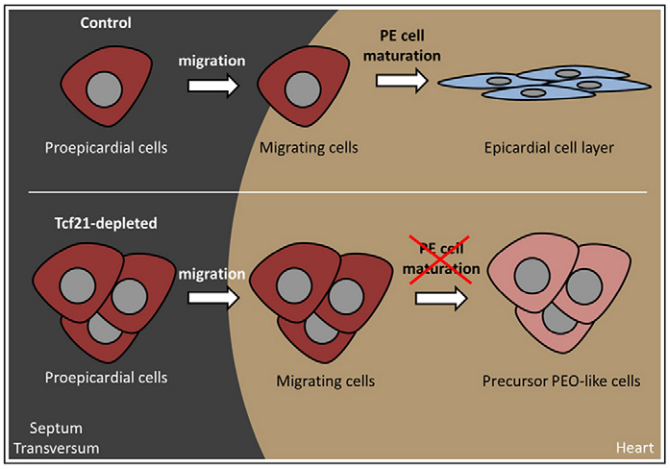

Fig. 8. Model for the role of Tcf21 in proepicardial cell specification and maturation. In control embryos, PE cells migrate onto the heart surface and mature into the epithelial-like epicardium (top panel). In the absence of Tcf21, PE cell numbers are increased and these cells retain their precursor cell characteristics upon migration onto the heart (bottom panel).

pluripotent precursor cells, the PEO, which our work in *Xenopus* has demonstrated to be a highly dynamic structure during its maturation into the epicardium. The cellular changes associated with maturation involve a transition between a migratory mesothelial-like PE cell to a more mature polarized and adherent epithelial epicardial sheet. To better understand these processes we have investigated the transcriptional regulation of epicardium formation. Our cellular, biochemical and molecular data are all consistent with a role for Tcf21 in PE specification and maturation.

Tcf21 and epicardial cell fate

Fate mapping of the epicardium has demonstrated that it can give rise to cardiac fibroblasts and smooth muscle cells (Vrancken Peeters et al., 1999; Olivey et al., 2006; Acharya et al., 2011; Kikuchi et al., 2011; Acharya et al., 2012; Braitsch et al., 2012). Recent reports using the mouse model implied a role for Tcf21 in cell fate decisions, demonstrating a requirement for Tcf21 in the cardiac fibroblast lineage (Acharya et al., 2012; Braitsch et al., 2012). Consistent with our findings, both groups showed a morphological defect in epicardial integrity in the absence of Tcf21. However, dissimilar theories were put forward to explain the preferential loss of the cardiac fibroblast lineage, with the absence being attributed to either a defect in epicardial EMT (Acharya et al., 2012) or a premature differentiation of epicardial cells into smooth muscle at the heart surface (Braitsch et al., 2012).

Based on our cellular, biochemical and molecular findings we favor an alternative model by which Tcf21 plays an earlier role in the correct specification of PE cells. In this model, in the absence of Tcf21 function, epicardial cell number is increased, an observation that bares resemblance to the findings in mouse of an increased number of *Tcf21*-null lineage-traced epicardial cells (Acharya et al., 2012), as well as an increase in rounded cell condensates surrounding the uteric bud in *Tcf21*-null mice (Quaggin et al., 1999; Cui et al., 2003), suggesting a conserved mechanism between the tissues. Furthermore, the Tcf21-depleted cells remain in an immature precursor state, which is reflected by the cells exhibiting a more PE-like and migratory state. As such, Tcf21-depleted epicardial cells fail to attain complete contact with, or to adhere to, the surface of the heart. This in turn leads to a failure of Tcf21-depleted cells to receive the necessary instructive signals to invade the myocardium and to fully differentiate into respective terminal cardiac cell types, including cardiac fibroblasts.

In addition, although the depth of analysis provided in the mouse models was extensive, we are cautious that markers of smooth muscle, primarily actin-binding proteins, have also been identified in other cardiac populations and migratory mesenchymal cell types (Tarin and Sturdee, 1971; Li et al., 1996; Miano and Olson, 1996; Nakajima et al., 1997; Langlois et al., 2010; Thompson et al., 2012), which could include the precursor PE cells. Our data therefore highlight a unique earlier mechanism whereby precursor epicardial cell specification is coordinated by Tcf21, with its depletion resulting in the phenotypes described in both *Xenopus* and mouse and leading ultimately to the later observed deficiencies in EPDC lineages.

Tcf21 interactions with transcriptional regulatory proteins

Transcriptional assays and electrophoretic mobility shift assays have shown Tcf21 to have transcriptional activity, both activating and repressive, in a number of *in vitro* systems (Hidai et al., 1998; Miyagishi et al., 2000; Funato et al., 2003; Cui et al., 2005; Hong et al., 2005; Plotkin and Mudunuri, 2008). However, only three potential direct transcriptional targets of Tcf21 have been reported, namely the genes encoding Muscle creatine kinase, Androgen receptor and Kisspeptin-1 (Kiss1) (Funato et al., 2003; Hong et al., 2005; Arab et al., 2011). Interestingly, Tcf21 silencing and its effects on *Kiss1* transcription have been linked to cancer cell metastasis and increased cell migration (Arab et al., 2011). Our mass spectrometry experiments confirmed the interaction of Tcf21 with Tcf12, a known class I bHLH heterodimeric partner of Tcf21 (Hidai et al., 1998; Lu et al., 1998; Arab et al., 2011) that has been implicated in cancer metastasis and the maintenance of pluripotency (Uittenbogaard and Chiaramello, 2002; Lee et al., 2012). Interestingly, our results also reveal interactions with HDAC2, Pbx1 and Ctbp2, suggesting that Tcf21 can act as a transcriptional repressor by functioning to locally remodel chromatin. The finding that HDAC2 associates with Tcf21 might indicate that Tcf21 can interact with HDAC-containing complexes in a context-dependent manner (Zupkovitz et al., 2006; Dovey et al., 2010; Kurosawa et al., 2010; Jurkin et al., 2011).

Additionally, our data show an association of Tcf21 with Pbx1 and Ctbp2, two proteins with an established role in heart development and disease (Katsanis and Fisher, 1998; Hildebrand and Soriano, 2002; Chinnadurai, 2003; Chang et al., 2008; Stankunas et al., 2008; Arrington et al., 2012). Moreover, *Pbx1*, which encodes a homeodomain transcription factor, has been demonstrated to genetically interact with *Tcf21* to control spleen development (Brendolan et al., 2005) and, in complex with the bHLH transcription factor Tcf3, has been implicated in acute lymphoblastic leukemia (McWhirter et al., 1997; Waurzyniak et al., 1998; Knoepfler et al., 1999). Thus, our data suggest that a common set of Tcf21-interacting proteins might function in a broad set of developmental processes and disease states.

Proepicardial specification and competence to differentiate

An understanding of the mechanisms that govern the specification of the PEO is of increasing importance with regards to epicardial cell pluripotency and their ability to repopulate and repair an infarcted adult heart. Given the paucity in known epicardial genes and useful epicardial-specific enhancers, and the lack of Tcf21

transcriptional targets (direct or non-direct) in the epicardium, it is interesting to speculate about the potential role of the nine genetic markers of the proepicardial lineage identified in our study. Compellingly, these genes have previously been ascribed roles in modulating ECM remodeling, cell adhesion, migration and epithelial-mesenchymal interactions, and frequently in the context of human malignancies and diseases, including Alzheimer's, Noonan syndrome and cardiovascular disorders (Jones and Jomary, 2002; Ny et al., 2002; Lin et al., 2005; Plaisier et al., 2005; Lin et al., 2006; Hu et al., 2007; Wei et al., 2009; Lee et al., 2010; Liu et al., 2010; Mehta and Parker, 2010; Fan et al., 2011; Tsai et al., 2011). Furthermore, with current data showing that differential transcriptional competency within the PEO can give rise to various EPDC populations (Mikawa and Gourdie, 1996; Männer, 1999; Jenkins et al., 2005; Guadix et al., 2006; Smith et al., 2011; Acharya et al., 2012; Katz et al., 2012) and recent findings that adult resident cardiac stem cells have a PEO origin (Chong et al., 2011), further investigation into the function of these genes during epicardium formation might provide a better understanding of their roles during normal cardiac development and human disease.

Acknowledgements
We are extremely grateful to the Faculty of Microscopy Services Laboratory at UNC for help with microscopy; John Wallingford for helpful discussions and critical reading of manuscript; and Nirav Amin, Erin Osborne, Hemant Kelkar, James Minchin and Taejoon Kwon for guidance in RNA-seq and for statistical analysis advice. The antibodies against vimentin and cytokeratin type II (developed by M. Klymkowsky) and tropomyosin (developed by Jim Jung-Ching Lin) were obtained from the Developmental Studies Hybridoma Bank, developed under the auspices of the NICHD and maintained by the University of Iowa, Department of Biological Sciences, Iowa City, IA 52242, USA.

Funding
We are thankful for funding from the National Institutes of Health [R01 HL 112618-01 to F.L.C. and National Institute on Drug Abuse grant DP1DA026192 to I.M.C.]; and the Human Frontier Science Program Organization [award RGY0079/2009-C to I.M.C.]. Deposited in PMC for release after 12 months.

Competing interests statement
The authors declare no competing financial interests.

Supplementary material
Supplementary material available online at
http://dev.biologists.org/lookup/suppl/doi:10.1242/dev.093385/-/DC1

References

Acharya, A., Baek, S. T., Banfi, S., Eskiocak, B. and Tallquist, M. D. (2011). Efficient inducible Cre-mediated recombination in Tcf21 cell lineages in the heart and kidney. *Genesis* **49**, 870-877.
Acharya, A., Baek, S. T., Huang, G., Eskiocak, B., Goetsch, S., Sung, C. Y., Banfi, S., Sauer, M. F., Olsen, G. S., Duffield, J. S. et al. (2012). The bHLH transcription factor Tcf21 is required for lineage-specific EMT of cardiac fibroblast progenitors. *Development* **139**, 2139-2149.
Afouda, B. A. and Hoppler, S. (2009). Xenopus explants as an experimental model system for studying heart development. *Trends Cardiovasc. Med.* **19**, 220-226.
Arab, K., Smith, L. T., Gast, A., Weichenhan, D., Huang, J. P., Claus, R., Hielscher, T., Espinosa, A. V., Ringel, M. D., Morrison, C. D. et al. (2011). Epigenetic deregulation of TCF21 inhibits metastasis suppressor KISS1 in metastatic melanoma. *Carcinogenesis* **32**, 1467-1473.
Arrington, C. B., Dowse, B. R., Bleyl, S. B. and Bowles, N. E. (2012). Non-synonymous variants in pre-B cell leukemia homeobox (PBX) genes are associated with congenital heart defects. *Eur. J. Med. Genet.* **55**, 235-237.
Bartlett, H. L. and Weeks, D. L. (2008). Lessons from the lily pad: using Xenopus to understand heart disease. *Drug Discov. Today Dis. Models* **5**, 141-146.
Bartlett, H. L., Sutherland, L., Kolker, S. J., Welp, C., Tajchman, U., Desmarais, V. and Weeks, D. L. (2007). Transient early embryonic expression of Nkx2-5 mutations linked to congenital heart defects in human causes heart defects in Xenopus laevis. *Dev. Dyn.* **236**, 2475-2484.
Begemann, G., Gibert, Y., Meyer, A. and Ingham, P. W. (2002). Cloning of zebrafish T-box genes tbx15 and tbx18 and their expression during embryonic development. *Mech. Dev.* **114**, 137-141.
Bowes, J. B., Snyder, K. A., Segerdell, E., Gibb, R., Jarabek, C., Noumen, E., Pollet, N. and Vize, P. D. (2008). Xenbase: a Xenopus biology and genomics resource. *Nucleic Acids Res.* **36**, D761-D767.
Braitsch, C. M., Combs, M. D., Quaggin, S. E. and Yutzey, K. E. (2012). Pod1/Tcf21 is regulated by retinoic acid signaling and inhibits differentiation of epicardium-derived cells into smooth muscle in the developing heart. *Dev. Biol.* **368**, 345-357.
Brendolan, A., Ferretti, E., Salsi, V., Moses, K., Quaggin, S., Blasi, F., Cleary, M. L. and Selleri, L. (2005). A Pbx1-dependent genetic and transcriptional network regulates spleen ontogeny. *Development* **132**, 3113-3126.
Brown, D. D., Binder, O., Pagratis, M., Parr, B. A. and Conlon, F. L. (2003). Developmental expression of the Xenopus laevis Tbx20 orthologue. *Dev. Genes Evol.* **212**, 604-607.
Brown, D. D., Martz, S. N., Binder, O., Goetz, S. C., Price, B. M., Smith, J. C. and Conlon, F. L. (2005). Tbx5 and Tbx20 act synergistically to control vertebrate heart morphogenesis. *Development* **132**, 553-563.
Brown, D. D., Christine, K. S., Showell, C. and Conlon, F. L. (2007). Small heat shock protein Hsp27 is required for proper heart tube formation. *Genesis* **45**, 667-678.
Bussen, M., Petry, M., Schuster-Gossler, K., Leitges, M., Gossler, A. and Kispert, A. (2004). The T-box transcription factor Tbx18 maintains the separation of anterior and posterior somite compartments. *Genes Dev.* **18**, 1209-1221.
Carmona, R., González-Iriarte, M., Pérez-Pomares, J. M. and Muñoz-Chápuli, R. (2001). Localization of the Wilm's tumour protein WT1 in avian embryos. *Cell Tissue Res.* **303**, 173-186.
Carroll, T. J. and Vize, P. D. (1996). Wilms' tumor suppressor gene is involved in the development of disparate kidney forms: evidence from expression in the Xenopus pronephros. *Dev. Dyn.* **206**, 131-138.
Chang, C. P., Stankunas, K., Shang, C., Kao, S. C., Twu, K. Y. and Cleary, M. L. (2008). Pbx1 functions in distinct regulatory networks to pattern the great arteries and cardiac outflow tract. *Development* **135**, 3577-3586.
Chinnadurai, G. (2003). CtBP family proteins: more than transcriptional corepressors. *BioEssays* **25**, 9-12.
Chong, J. J., Chandrakanthan, V., Xaymardan, M., Asli, N. S., Li, J., Ahmed, I., Heffernan, C., Menon, M. K., Scarlett, C. J., Rashidianfar, A. et al. (2011). Adult cardiac-resident MSC-like stem cells with a proepicardial origin. *Cell Stem Cell* **9**, 527-540.
Christine, K. S. and Conlon, F. L. (2008). Vertebrate CASTOR is required for differentiation of cardiac precursor cells at the ventral midline. *Dev. Cell* **14**, 616-623.
Christoffels, V. M., Mommersteeg, M. T., Trowe, M. O., Prall, O. W., de Gier-de Vries, C., Soufan, A. T., Bussen, M., Schuster-Gossler, K., Harvey, R. P., Moorman, A. F. et al. (2006). Formation of the venous pole of the heart from an Nkx2-5-negative precursor population requires Tbx18. *Circ. Res.* **98**, 1555-1563.
Compton, L. A., Potash, D. A., Mundell, N. A. and Barnett, J. V. (2006). Transforming growth factor-beta induces loss of epithelial character and smooth muscle cell differentiation in epicardial cells. *Dev. Dyn.* **235**, 82-93.
Conlon, F. L., Miteva, Y., Kaltenbrun, E., Waldron, L., Greco, T. M. and Cristea, I. M. (2012). Immunoisolation of protein complexes from Xenopus. *Methods Mol. Biol.* **917**, 369-390.
Conway, S. J., Firulli, B. and Firulli, A. B. (2010). A bHLH code for cardiac morphogenesis. *Pediatr. Cardiol.* **31**, 318-324.
Cristea, I. M., Williams, R., Chait, B. T. and Rout, M. P. (2005). Fluorescent proteins as proteomic probes. *Mol. Cell. Proteomics* **4**, 1933-1941.
Cui, S., Schwartz, L. and Quaggin, S. E. (2003). Pod1 is required in stromal cells for glomerulogenesis. *Dev. Dyn.* **226**, 512-522.
Cui, S., Li, C., Ema, M., Weinstein, J. and Quaggin, S. E. (2005). Rapid isolation of glomeruli coupled with gene expression profiling identifies downstream targets in Pod1 knockout mice. *J. Am. Soc. Nephrol.* **16**, 3247-3255.
Dent, J. A., Polson, A. G. and Klymkowsky, M. W. (1989). A whole-mount immunocytochemical analysis of the expression of the intermediate filament protein vimentin in Xenopus. *Development* **105**, 61-74.
Dettman, R. W., Pae, S. H., Morabito, C. and Bristow, J. (2003). Inhibition of alpha4-integrin stimulates epicardial-mesenchymal transformation and alters migration and cell fate of epicardially derived mesenchyme. *Dev. Biol.* **257**, 315-328.
Dovey, O. M., Foster, C. T. and Cowley, S. M. (2010). Histone deacetylase 1 (HDAC1), but not HDAC2, controls embryonic stem cell differentiation. *Proc. Natl. Acad. Sci. USA* **107**, 8242-8247.
Eden, E., Lipson, D., Yogev, S. and Yakhini, Z. (2007). Discovering motifs in ranked lists of DNA sequences. *PLoS Comput. Biol.* **3**, e39.
Eden, E., Navon, R., Steinfeld, I., Lipson, D. and Yakhini, Z. (2009). GOrilla: a tool for discovery and visualization of enriched GO terms in ranked gene lists. *BMC Bioinformatics* **10**, 48.
Evans, S. M., Yelon, D., Conlon, F. L. and Kirby, M. L. (2010). Myocardial lineage development. *Circ. Res.* **107**, 1428-1444.

Fan, C., Fu, Z., Su, Q., Angelini, D. J., Van Eyk, J. and Johns, R. A. (2011). S100A11 mediates hypoxia-induced mitogenic factor (HIMF)-induced smooth muscle cell migration, vesicular exocytosis, and nuclear activation. *Mol. Cell. Proteomics* **10**, M110.000901.
Funato, N., Ohyama, K., Kuroda, T. and Nakamura, M. (2003). Basic helix-loop-helix transcription factor epicardin/capsulin/Pod-1 suppresses differentiation by negative regulation of transcription. *J. Biol. Chem.* **278**, 7486-7493.
Garriock, R. J., D'Agostino, S. L., Pilcher, K. C. and Krieg, P. A. (2005). Wnt11-R, a protein closely related to mammalian Wnt11, is required for heart morphogenesis in Xenopus. *Dev. Biol.* **279**, 179-192.
Gessert, S. and Kühl, M. (2009). Comparative gene expression analysis and fate mapping studies suggest an early segregation of cardiogenic lineages in Xenopus laevis. *Dev. Biol.* **334**, 395-408.
Ghosh, S., Marquardt, T., Thaler, J. P., Carter, N., Andrews, S. E., Pfaff, S. L. and Hunter, T. (2008). Instructive role of aPKCzeta subcellular localization in the assembly of adherens junctions in neural progenitors. *Proc. Natl. Acad. Sci. USA* **105**, 335-340.
Gittenberger-de Groot, A. C., Winter, E. M., Bartelings, M. M., Goumans, M. J., DeRuiter, M. C. and Poelmann, R. E. (2012). The arterial and cardiac epicardium in development, disease and repair. *Differentiation* **84**, 41-53.
Goetz, S. C., Brown, D. D. and Conlon, F. L. (2006). TBX5 is required for embryonic cardiac cell cycle progression. *Development* **133**, 2575-2584.
Gormley, J. P. and Nascone-Yoder, N. M. (2003). Left and right contributions to the Xenopus heart: implications for asymmetric morphogenesis. *Dev. Genes Evol.* **213**, 390-398.
Greco, T. M., Yu, F., Guise, A. J. and Cristea, I. M. (2011). Nuclear import of histone deacetylase 5 by requisite nuclear localization signal phosphorylation. *Mol. Cell. Proteomics* **10**, M110.004317.
Greco, T. M., Miteva, Y., Conlon, F. L. and Cristea, I. M. (2012). Complementary proteomic analysis of protein complexes. *Methods Mol. Biol.* **917**, 391-407.
Griswold, S. L., Sajja, K. C., Jang, C. W. and Behringer, R. R. (2011). Generation and characterization of iUBC-KikGR photoconvertible transgenic mice for live time-lapse imaging during development. *Genesis* **49**, 591-598.
Guadix, J. A., Carmona, R., Muñoz-Chápuli, R. and Pérez-Pomares, J. M. (2006). In vivo and in vitro analysis of the vasculogenic potential of avian proepicardial and epicardial cells. *Dev. Dyn.* **235**, 1014-1026.
Haenig, B. and Kispert, A. (2004). Analysis of TBX18 expression in chick embryos. *Dev. Genes Evol.* **214**, 407-411.
Harland, R. M. (1991). In situ hybridization: an improved whole-mount method for Xenopus embryos. *Methods Cell Biol.* **36**, 685-695.
Hidai, H., Bardales, R., Goodwin, R., Quertermous, T. and Quertermous, E. E. (1998). Cloning of capsulin, a basic helix-loop-helix factor expressed in progenitor cells of the pericardium and the coronary arteries. *Mech. Dev.* **73**, 33-43.
Hildebrand, J. D. and Soriano, P. (2002). Overlapping and unique roles for C-terminal binding protein 1 (CtBP1) and CtBP2 during mouse development. *Mol. Cell. Biol.* **22**, 5296-5307.
Hirose, T., Karasawa, M., Sugitani, Y., Fujisawa, M., Akimoto, K., Ohno, S. and Noda, T. (2006). PAR3 is essential for cyst-mediated epicardial development by establishing apical cortical domains. *Development* **133**, 1389-1398.
Hong, C. Y., Gong, E. Y., Kim, K., Suh, J. H., Ko, H. M., Lee, H. J., Choi, H. S. and Lee, K. (2005). Modulation of the expression and transactivation of androgen receptor by the basic helix-loop-helix transcription factor Pod-1 through recruitment of histone deacetylase 1. *Mol. Endocrinol.* **19**, 2245-2257.
Hu, K., Wu, C., Mars, W. M. and Liu, Y. (2007). Tissue-type plasminogen activator promotes murine myofibroblast activation through LDL receptor-related protein 1-mediated integrin signaling. *J. Clin. Invest.* **117**, 3821-3832.
Ishii, Y., Langberg, J. D., Hurtado, R., Lee, S. and Mikawa, T. (2007). Induction of proepicardial marker gene expression by the liver bud. *Development* **134**, 3627-3637.
Ishii, Y., Garriock, R. J., Navetta, A. M., Coughlin, L. E. and Mikawa, T. (2010). BMP signals promote proepicardial protrusion necessary for recruitment of coronary vessel and epicardial progenitors to the heart. *Dev. Cell* **19**, 307-316.
Izumi, Y., Hirose, T., Tamai, Y., Hirai, S., Nagashima, Y., Fujimoto, T., Tabuse, Y., Kemphues, K. J. and Ohno, S. (1998). An atypical PKC directly associates and colocalizes at the epithelial tight junction with ASIP, a mammalian homologue of Caenorhabditis elegans polarity protein PAR-3. *J. Cell Biol.* **143**, 95-106.
Jahr, M., Schlueter, J., Brand, T. and Männer, J. (2008). Development of the proepicardium in Xenopus laevis. *Dev. Dyn.* **237**, 3088-3096.
Jenkins, S. J., Hutson, D. R. and Kubalak, S. W. (2005). Analysis of the proepicardium-epicardium transition during the malformation of the RXRalpha–/– epicardium. *Dev. Dyn.* **233**, 1091-1101.
Jones, S. E. and Jomary, C. (2002). Clusterin. *Int. J. Biochem. Cell Biol.* **34**, 427-431.
Jurkin, J., Zupkovitz, G., Lagger, S., Grausenburger, R., Hagelkruys, A., Kenner, L. and Seiser, C. (2011). Distinct and redundant functions of histone deacetylases HDAC1 and HDAC2 in proliferation and tumorigenesis. *Cell Cycle* **10**, 406-412.
Kálmán, F., Virágh, S. and Módis, L. (1995). Cell surface glycoconjugates and the extracellular matrix of the developing mouse embryo epicardium. *Anat. Embryol. (Berl.)* **191**, 451-464.
Kaltenbrun, E., Tandon, P., Amin, N. M., Waldron, L., Showell, C. and Conlon, F. L. (2011). Xenopus: An emerging model for studying congenital heart disease. *Birth Defects Res. A Clin. Mol. Teratol.* **91**, 495-510.
Kang, J., Gu, Y., Li, P., Johnson, B. L., Sucov, H. M. and Thomas, P. S. (2008). PDGF-A as an epicardial mitogen during heart development. *Dev. Dyn.* **237**, 692-701.
Katsanis, N. and Fisher, E. M. (1998). A novel C-terminal binding protein (CTBP2) is closely related to CTBP1, an adenovirus E1A-binding protein, and maps to human chromosome 21q21.3. *Genomics* **47**, 294-299.
Katz, T. C., Singh, M. K., Degenhardt, K., Rivera-Feliciano, J., Johnson, R. L., Epstein, J. A. and Tabin, C. J. (2012). Distinct compartments of the proepicardial organ give rise to coronary vascular endothelial cells. *Dev. Cell* **22**, 639-650.
Kikuchi, K., Gupta, V., Wang, J., Holdway, J. E., Wills, A. A., Fang, Y. and Poss, K. D. (2011). tcf21+ epicardial cells adopt non-myocardial fates during zebrafish heart development and regeneration. *Development* **138**, 2895-2902.
Kirschner, K. M., Wagner, N., Wagner, K. D., Wellmann, S. and Scholz, H. (2006). The Wilms tumor suppressor Wt1 promotes cell adhesion through transcriptional activation of the alpha4integrin gene. *J. Biol. Chem.* **281**, 31930-31939.
Knoepfler, P. S., Bergstrom, D. A., Uetsuki, T., Dac-Korytko, I., Sun, Y. H., Wright, W. E., Tapscott, S. J. and Kamps, M. P. (1999). A conserved motif N-terminal to the DNA-binding domains of myogenic bHLH transcription factors mediates cooperative DNA binding with pbx-Meis1/Prep1. *Nucleic Acids Res.* **27**, 3752-3767.
Komiyama, M., Ito, K. and Shimada, Y. (1987). Origin and development of the epicardium in the mouse embryo. *Anat. Embryol. (Berl.)* **176**, 183-189.
Kovi, R. C., Paliwal, S., Pande, S. and Grossman, S. R. (2010). An ARF/CtBP2 complex regulates BH3-only gene expression and p53-independent apoptosis. *Cell Death Differ.* **17**, 513-521.
Kraus, F., Haenig, B. and Kispert, A. (2001). Cloning and expression analysis of the mouse T-box gene Tbx18. *Mech. Dev.* **100**, 83-86.
Kroll, K. L. and Amaya, E. (1996). Transgenic Xenopus embryos from sperm nuclear transplantations reveal FGF signaling requirements during gastrulation. *Development* **122**, 3173-3183.
Kurosawa, K., Lin, W. and Ohta, K. (2010). Distinct roles of HDAC1 and HDAC2 in transcription and recombination at the immunoglobulin loci in the chicken B cell line DT40. *J. Biochem.* **148**, 201-207.
Langdon, Y. G., Goetz, S. C., Berg, A. E., Swanik, J. T. and Conlon, F. L. (2007). SHP-2 is required for the maintenance of cardiac progenitors. *Development* **134**, 4119-4130.
Langdon, Y., Tandon, P., Paden, E., Duddy, J., Taylor, J. M. and Conlon, F. L. (2012). SHP-2 acts via ROCK to regulate the cardiac actin cytoskeleton. *Development* **139**, 948-957.
Langlois, D., Hneino, M., Bouazza, L., Parlakian, A., Sasaki, T., Bricca, G. and Li, J. Y. (2010). Conditional inactivation of TGF-β type II receptor in smooth muscle cells and epicardium causes lethal aortic and cardiac defects. *Transgenic Res.* **19**, 1069-1082.
Latinkić, B. V., Cooper, B., Towers, N., Sparrow, D., Kotecha, S. and Mohun, T. J. (2002). Distinct enhancers regulate skeletal and cardiac muscle-specific expression programs of the cardiac alpha-actin gene in Xenopus embryos. *Dev. Biol.* **245**, 57-70.
Lee, Y. C., Lin, K. P., Chang, M. H., Liao, Y. C., Tsai, C. P., Liao, K. K. and Soong, B. W. (2010). Cellular characterization of MPZ mutations presenting with diverse clinical phenotypes. *J. Neurol.* **257**, 1661-1668.
Lee, C. C., Chen, W. S., Chen, C. C., Chen, L. L., Lin, Y. S., Fan, C. S. and Huang, T. S. (2012). TCF12 protein functions as transcriptional repressor of E-cadherin, and its overexpression is correlated with metastasis of colorectal cancer. *J. Biol. Chem.* **287**, 2798-2809.
Lepilina, A., Coon, A. N., Kikuchi, K., Holdway, J. E., Roberts, R. W., Burns, C. G. and Poss, K. D. (2006). A dynamic epicardial injury response supports progenitor cell activity during zebrafish heart regeneration. *Cell* **127**, 607-619.
Li, L., Miano, J. M., Cserjesi, P. and Olson, E. N. (1996). SM22 alpha, a marker of adult smooth muscle, is expressed in multiple myogenic lineages during embryogenesis. *Circ. Res.* **78**, 188-195.
Lie-Venema, H., van den Akker, N. M., Bax, N. A., Winter, E. M., Maas, S., Kekarainen, T., Hoeben, R. C., deRuiter, M. C., Poelmann, R. E. and Gittenberger-de Groot, A. C. (2007). Origin, fate, and function of epicardium-derived cells (EPDCs) in normal and abnormal cardiac development. *ScientificWorldJournal* **7**, 1777-1798.
Limana, F., Zacheo, A., Mocini, D., Mangoni, A., Borsellino, G., Diamantini, A., De Mori, R., Battistini, L., Vigna, E., Santini, M. et al. (2007). Identification of myocardial and vascular precursor cells in human and mouse epicardium. *Circ. Res.* **101**, 1255-1265.
Limana, F., Bertolami, C., Mangoni, A., Di Carlo, A., Avitabile, D., Mocini, D., Iannelli, P., De Mori, R., Marchetti, C., Pozzoli, O. et al. (2010). Myocardial

infarction induces embryonic reprogramming of epicardial c-kit(+) cells: role of the pericardial fluid. *J. Mol. Cell. Cardiol.* **48**, 609-618.
Lin, J., Patel, S. R., Cheng, X., Cho, E. A., Levitan, I., Ullenbruch, M., Phan, S. H., Park, J. M. and Dressler, G. R. (2005). Kielin/chordin-like protein, a novel enhancer of BMP signaling, attenuates renal fibrotic disease. *Nat. Med.* **11**, 387-393.
Lin, J., Patel, S. R., Wang, M. and Dressler, G. R. (2006). The cysteine-rich domain protein KCP is a suppressor of transforming growth factor beta/activin signaling in renal epithelia. *Mol. Cell. Biol.* **26**, 4577-4585.
Liu, J. and Stainier, D. Y. (2010). Tbx5 and Bmp signaling are essential for proepicardium specification in zebrafish. *Circ. Res.* **106**, 1818-1828.
Liu, X. G., Wang, X. P., Li, W. F., Yang, S., Zhou, X., Li, S. J., Li, X. J., Hao, D. Y. and Fan, Z. M. (2010). Ca^{2+}-binding protein S100A11: a novel diagnostic marker for breast carcinoma. *Oncol. Rep.* **23**, 1301-1308.
Lu, J., Richardson, J. A. and Olson, E. N. (1998). Capsulin: a novel bHLH transcription factor expressed in epicardial progenitors and mesenchyme of visceral organs. *Mech. Dev.* **73**, 23-32.
Lu, J., Chang, P., Richardson, J. A., Gan, L., Weiler, H. and Olson, E. N. (2000). The basic helix-loop-helix transcription factor capsulin controls spleen organogenesis. *Proc. Natl. Acad. Sci. USA* **97**, 9525-9530.
Mandel, E. M., Kaltenbrun, E., Callis, T. E., Zeng, X. X., Marques, S. R., Yelon, D., Wang, D. Z. and Conlon, F. L. (2010). The BMP pathway acts to directly regulate Tbx20 in the developing heart. *Development* **137**, 1919-1929.
Männer, J. (1999). Does the subepicardial mesenchyme contribute myocardioblasts to the myocardium of the chick embryo heart? A quail-chick chimera study tracing the fate of the epicardial primordium. *Anat. Rec.* **255**, 212-226.
Martínez-Estrada, O. M., Lettice, L. A., Essafi, A., Guadix, J. A., Slight, J., Velecela, V., Hall, E., Reichmann, J., Devenney, P. S., Hohenstein, P. et al. (2010). Wt1 is required for cardiovascular progenitor cell formation through transcriptional control of Snail and E-cadherin. *Nat. Genet.* **42**, 89-93.
Massari, M. E. and Murre, C. (2000). Helix-loop-helix proteins: regulators of transcription in eucaryotic organisms. *Mol. Cell. Biol.* **20**, 429-440.
McWhirter, J. R., Goulding, M., Weiner, J. A., Chun, J. and Murre, C. (1997). A novel fibroblast growth factor gene expressed in the developing nervous system is a downstream target of the chimeric homeodomain oncoprotein E2A-Pbx1. *Development* **124**, 3221-3232.
Mehta, P. and Parker, R. I. (2010). Imbalance of plasminogen activator inhibitor type-1 (PAI-1) and tissue plasminogen activator (t-PA) activity in patients with Noonan syndrome. *J. Pediatr. Hematol. Oncol.* **32**, 532-536.
Miano, J. M. and Olson, E. N. (1996). Expression of the smooth muscle cell calponin gene marks the early cardiac and smooth muscle cell lineages during mouse embryogenesis. *J. Biol. Chem.* **271**, 7095-7103.
Mikawa, T. and Gourdie, R. G. (1996). Pericardial mesoderm generates a population of coronary smooth muscle cells migrating into the heart along with ingrowth of the epicardial organ. *Dev. Biol.* **174**, 221-232.
Miyagishi, M., Hatta, M., Ohshima, T., Ishida, J., Fujii, R., Nakajima, T. and Fukamizu, A. (2000). Cell type-dependent transactivation or repression of mesoderm-restricted basic helix-loop-helix protein, POD-1/Capsulin. *Mol. Cell. Biochem.* **205**, 141-147.
Mohun, T., Orford, R. and Shang, C. (2003). The origins of cardiac tissue in the amphibian, Xenopus laevis. *Trends Cardiovasc. Med.* **13**, 244-248.
Moore, A. W., Schedl, A., McInnes, L., Doyle, M., Hecksher-Sorensen, J. and Hastie, N. D. (1998). YAC transgenic analysis reveals Wilms' tumour 1 gene activity in the proliferating coelomic epithelium, developing diaphragm and limb. *Mech. Dev.* **79**, 169-184.
Moore, A. W., McInnes, L., Kreidberg, J., Hastie, N. D. and Schedl, A. (1999). YAC complementation shows a requirement for Wt1 in the development of epicardium, adrenal gland and throughout nephrogenesis. *Development* **126**, 1845-1857.
Munson, C., Huisken, J., Bit-Avragim, N., Kuo, T., Dong, P. D., Ober, E. A., Verkade, H., Abdelilah-Seyfried, S. and Stainier, D. Y. (2008). Regulation of neurocoel morphogenesis by Pard6 gamma b. *Dev. Biol.* **324**, 41-54.
Nahirney, P. C., Mikawa, T. and Fischman, D. A. (2003). Evidence for an extracellular matrix bridge guiding proepicardial cell migration to the myocardium of chick embryos. *Dev. Dyn.* **227**, 511-523.
Nakajima, Y., Mironov, V., Yamagishi, T., Nakamura, H. and Markwald, R. R. (1997). Expression of smooth muscle alpha-actin in mesenchymal cells during formation of avian endocardial cushion tissue: a role for transforming growth factor beta3. *Dev. Dyn.* **209**, 296-309.
Nieuwkoop, P. D. and Faber, J. (1967). *Normal Table of Xenopus laevis (Daudin).* Amsterdam: North-Holland Publishing.
Nowotschin, S. and Hadjantonakis, A. K. (2009). Use of KikGR a photoconvertible green-to-red fluorescent protein for cell labeling and lineage analysis in ES cells and mouse embryos. *BMC Dev. Biol.* **9**, 49.
Ny, T., Wahlberg, P. and Brändström, I. J. (2002). Matrix remodeling in the ovary: regulation and functional role of the plasminogen activator and matrix metalloproteinase systems. *Mol. Cell. Endocrinol.* **187**, 29-38.
Olivey, H. E., Mundell, N. A., Austin, A. F. and Barnett, J. V. (2006). Transforming growth factor-beta stimulates epithelial-mesenchymal transformation in the proepicardium. *Dev. Dyn.* **235**, 50-59.
Pae, S. H., Dokic, D. and Dettman, R. W. (2008). Communication between integrin receptors facilitates epicardial cell adhesion and matrix organization. *Dev. Dyn.* **237**, 962-978.
Pérez-Pomares, J. M. and de la Pompa, J. L. (2011). Signaling during epicardium and coronary vessel development. *Circ. Res.* **109**, 1429-1442.
Pinco, K. A., Liu, S. and Yang, J. T. (2001). alpha4 integrin is expressed in a subset of cranial neural crest cells and in epicardial progenitor cells during early mouse development. *Mech. Dev.* **100**, 99-103.
Plaisier, E., Mougenot, B., Verpont, M. C., Jouanneau, C., Archelos, J. J., Martini, R., Kerjaschki, D. and Ronco, P. (2005). Glomerular permeability is altered by loss of P0, a myelin protein expressed in glomerular epithelial cells. *J. Am. Soc. Nephrol.* **16**, 3350-3356.
Plotkin, M. and Mudunuri, V. (2008). Pod1 induces myofibroblast differentiation in mesenchymal progenitor cells from mouse kidney. *J. Cell. Biochem.* **103**, 675-690.
Pombal, M. A., Carmona, R., Megías, M., Ruiz, A., Pérez-Pomares, J. M. and Muñoz-Chápuli, R. (2008). Epicardial development in lamprey supports an evolutionary origin of the vertebrate epicardium from an ancestral pronephric external glomerulus. *Evol. Dev.* **10**, 210-216.
Quaggin, S. E., Vanden Heuvel, G. B. and Igarashi, P. (1998). Pod-1, a mesoderm-specific basic-helix-loop-helix protein expressed in mesenchymal and glomerular epithelial cells in the developing kidney. *Mech. Dev.* **71**, 37-48.
Quaggin, S. E., Schwartz, L., Cui, S., Igarashi, P., Deimling, J., Post, M. and Rossant, J. (1999). The basic-helix-loop-helix protein pod1 is critically important for kidney and lung organogenesis. *Development* **126**, 5771-5783.
Ramos, C., Becerril, C., Montaño, M., García-De-Alba, C., Ramírez, R., Checa, M., Pardo, A. and Selman, M. (2010). FGF-1 reverts epithelial-mesenchymal transition induced by TGF-beta1 through MAPK/ERK kinase pathway. *Am. J. Physiol. Lung Cell. Mol. Physiol.* **299**, L222-L231.
Rappsilber, J., Mann, M. and Ishihama, Y. (2007). Protocol for micro-purification, enrichment, pre-fractionation and storage of peptides for proteomics using StageTips. *Nat. Protoc.* **2**, 1896-1906.
Ratajska, A., Czarnowska, E. and Ciszek, B. (2008). Embryonic development of the proepicardium and coronary vessels. *Int. J. Dev. Biol.* **52**, 229-236.
Ridelis, I., Schmidt, A., Teichmann, A., Furkert, J., Wiesner, B. and Schülein, R. (2012). Use of Kikume green-red fusions to study the influence of pharmacological chaperones on trafficking of G protein-coupled receptors. *FEBS Lett.* **586**, 784-791.
Schulte, I., Schlueter, J., Abu-Issa, R., Brand, T. and Männer, J. (2007). Morphological and molecular left-right asymmetries in the development of the proepicardium: a comparative analysis on mouse and chick embryos. *Dev. Dyn.* **236**, 684-695.
Serluca, F. C. (2008). Development of the proepicardial organ in the zebrafish. *Dev. Biol.* **315**, 18-27.
Shook, D. and Keller, R. (2003). Mechanisms, mechanics and function of epithelial-mesenchymal transitions in early development. *Mech. Dev.* **120**, 1351-1383.
Simrick, S., Massé, K. and Jones, E. A. (2005). Developmental expression of Pod 1 in Xenopus laevis. *Int. J. Dev. Biol.* **49**, 59-63.
Smagulova, F. O., Manuylov, N. L., Leach, L. L. and Tevosian, S. G. (2008). GATA4/FOG2 transcriptional complex regulates Lhx9 gene expression in murine heart development. *BMC Dev. Biol.* **8**, 67.
Smith, C. L., Baek, S. T., Sung, C. Y. and Tallquist, M. D. (2011). Epicardial-derived cell epithelial-to-mesenchymal transition and fate specification require PDGF receptor signaling. *Circ. Res.* **108**, e15-e26.
Stankunas, K., Shang, C., Twu, K. Y., Kao, S. C., Jenkins, N. A., Copeland, N. G., Sanyal, M., Selleri, L., Cleary, M. L. and Chang, C. P. (2008). Pbx/Meis deficiencies demonstrate multigenetic origins of congenital heart disease. *Circ. Res.* **103**, 702-709.
Supek, F., Bošnjak, M., Škunca, N. and Šmuc, T. (2011). REVIGO summarizes and visualizes long lists of gene ontology terms. *PLoS ONE* **6**, e21800.
Tamura, M., Kanno, Y., Chuma, S., Saito, T. and Nakatsuji, N. (2001). Pod-1/Capsulin shows a sex- and stage-dependent expression pattern in the mouse gonad development and represses expression of Ad4BP/SF-1. *Mech. Dev.* **102**, 135-144.
Tandon, P., Showell, C., Christine, K. and Conlon, F. L. (2012). Morpholino injection in Xenopus. *Methods Mol. Biol.* **843**, 29-46.
Tarin, D. and Sturdee, A. P. (1971). Early limb development of Xenopus laevis. *J. Embryol. Exp. Morphol.* **26**, 169-179.
Thompson, O., Moghraby, J. S., Ayscough, K. R. and Winder, S. J. (2012). Depletion of the actin bundling protein SM22/transgelin increases actin dynamics and enhances the tumourigenic phenotypes of cells. *BMC Cell Biol.* **13**, 1.
Torpey, N. P., Heasman, J. and Wylie, C. C. (1992). Distinct distribution of vimentin and cytokeratin in Xenopus oocytes and early embryos. *J. Cell Sci.* **101**, 151-160.

Trausch-Azar, J. S., Lingbeck, J., Ciechanover, A. and Schwartz, A. L. (2004). Ubiquitin-proteasome-mediated degradation of Id1 is modulated by MyoD. *J. Biol. Chem.* **279**, 32614-32619.
Tsai, F. M., Wu, C. C., Shyu, R. Y., Wang, C. H. and Jiang, S. Y. (2011). Tazarotene-induced gene 1 inhibits prostaglandin E2-stimulated HCT116 colon cancer cell growth. *J. Biomed. Sci.* **18**, 88.
Tsai, Y. C., Greco, T. M., Boonmee, A., Miteva, Y. and Cristea, I. M. (2012). Functional proteomics establishes the interaction of SIRT7 with chromatin remodeling complexes and expands its role in regulation of RNA polymerase I transcription. *Mol. Cell. Proteomics* **11**, 60-76.
Uittenbogaard, M. and Chiaramello, A. (2002). Expression of the bHLH transcription factor Tcf12 (ME1) gene is linked to the expansion of precursor cell populations during neurogenesis. *Brain Res. Gene Expr. Patterns* **1**, 115-121.
van Wijk, B., van den Berg, G., Abu-Issa, R., Barnett, P., van der Velden, S., Schmidt, M., Ruijter, J. M., Kirby, M. L., Moorman, A. F. and van den Hoff, M. J. (2009). Epicardium and myocardium separate from a common precursor pool by crosstalk between bone morphogenetic protein- and fibroblast growth factor-signaling pathways. *Circ. Res.* **105**, 431-441.
von Gise, A. and Pu, W. T. (2012). Endocardial and epicardial epithelial to mesenchymal transitions in heart development and disease. *Circ. Res.* **110**, 1628-1645.
Vrancken Peeters, M. P., Mentink, M. M., Poelmann, R. E. and Gittenberger-de Groot, A. C. (1995). Cytokeratins as a marker for epicardial formation in the quail embryo. *Anat. Embryol. (Berl.)* **191**, 503-508.
Vrancken Peeters, M. P., Gittenberger-de Groot, A. C., Mentink, M. M. and Poelmann, R. E. (1999). Smooth muscle cells and fibroblasts of the coronary arteries derive from epithelial-mesenchymal transformation of the epicardium. *Anat. Embryol. (Berl.)* **199**, 367-378.
Wallingford, J. B. (2010). Preparation of fixed Xenopus embryos for confocal imaging. *Cold Spring Harb. Protoc.* **2010**, pdb prot5426.
Warkman, A. S. and Krieg, P. A. (2007). Xenopus as a model system for vertebrate heart development. *Semin. Cell Dev. Biol.* **18**, 46-53.
Waurzyniak, B. J., Heerema, N., Sensel, M. G., Gaynon, P. S., Kraft, P., Sather, H. N., Chelstrom, L., Reaman, G. H. and Uckun, F. M. (1998). Distinct in vivo engraftment and growth patterns of t(1;19)+/E2A-PBX1+ and t(9;22)+/BCR-ABL+ human leukemia cells in SCID mice. *Leuk. Lymphoma* **32**, 77-87.
Wei, L., Xue, T., Wang, J., Chen, B., Lei, Y., Huang, Y., Wang, H. and Xin, X. (2009). Roles of clusterin in progression, chemoresistance and metastasis of human ovarian cancer. *Int. J. Cancer* **125**, 791-806.
Winter, E. M., Grauss, R. W., Hogers, B., van Tuyn, J., van der Geest, R., Lie-Venema, H., Steijn, R. V., Maas, S., DeRuiter, M. C., deVries, A. A. et al. (2007). Preservation of left ventricular function and attenuation of remodeling after transplantation of human epicardium-derived cells into the infarcted mouse heart. *Circulation* **116**, 917-927.
Winter, E. M., van Oorschot, A. A., Hogers, B., van der Graaf, L. M., Doevendans, P. A., Poelmann, R. E., Atsma, D. E., Gittenberger-de Groot, A. C. and Goumans, M. J. (2009). A new direction for cardiac regeneration therapy: application of synergistically acting epicardium-derived cells and cardiomyocyte progenitor cells. *Circ. Heart Fail.* **2**, 643-653.
Zhao, L. J., Subramanian, T. and Chinnadurai, G. (2006). Changes in C-terminal binding protein 2 (CtBP2) corepressor complex induced by E1A and modulation of E1A transcriptional activity by CtBP2. *J. Biol. Chem.* **281**, 36613-36623.
Zupkovitz, G., Tischler, J., Posch, M., Sadzak, I., Ramsauer, K., Egger, G., Grausenburger, R., Schweifer, N., Chiocca, S., Decker, T. et al. (2006). Negative and positive regulation of gene expression by mouse histone deacetylase 1. *Mol. Cell. Biol.* **26**, 7913-7928.